Applied Mathematical Modelling 44 (2017) 557–575

Contents lists available at ScienceDirect

Applied Mathematical Modelling

journal homepage: www.elsevier.com/locate/apm

Synchronization analysis through coupling mechanism in realistic neural models

Ranjit Kumar Upadhyay[a,*], Argha Mondal[a], M.A. Aziz-Alaoui[b]

[a] Department of Applied Mathematics, Indian Institute of Technology (Indian School of Mines), Dhanbad-826004, Jharkhand, INDIA
[b] UniHavre, LMAH, FR CNRS 3335, ISCN, Normandie University, 76600 Le Havre, France

ARTICLE INFO

Article history:
Received 16 July 2015
Revised 12 January 2017
Accepted 9 February 2017
Available online 20 February 2017

Keywords:
Generalized synchronization
Modified 3D Morris–Lecar neural model
OPCL method
Hindmarsh–Rose neural model
Bidirectional coupling

ABSTRACT

Synchronization which relates to the system's stability is important to many engineering and neural applications. In this paper, an attempt has been made to implement response synchronization using coupling mechanism for a class of nonlinear neural systems. We propose an OPCL (open-plus-closed-loop) coupling method to investigate the synchronization state of driver-response neural systems, and to understand how the behavior of these coupled systems depend on their inner dynamics. We have investigated a general method of coupling for generalized synchronization (GS) in 3D modified spiking and bursting Morris–Lecar (M-L) neural models. We have also presented the synchronized behavior of a network of four bursting Hindmarsh–Rose (H-R) neural oscillators using a bidirectional coupling mechanism. We can extend the coupling scheme to a network of N neural oscillators to reach the desired synchronous state. To make the investigations more promising, we consider another coupling method to a network of H-R oscillators using bidirectional ring type connections and present the effectiveness of the coupling scheme.

1. Introduction

Synchronization is a natural phenomenon in the real world system and it is experimented in research laboratory. Like different types of physical, chemical and biological systems; neural systems can synchronize and show collective behavior. Partial synchronous behavior in cortical region of brain areas may generate different brain waves such as alpha, beta, gamma and many more in EEG oscillations. Synchronization in neurons may cause the neurophysiological activity such as epilepsy. The concept of synchronization [1,2] in dynamical systems describes behavior of oscillatory systems, artificial systems and many spatial patterns of real world systems. We have also seen these types of phenomena in complex living system [3,4]. Control of synchronization in dynamical system particularly for the complex dynamics of brain control, both synchronization and desynchronization [5–7] are important. Many people have worked on the theory of identical oscillators to reduce the mathematical complexity for understanding the synchronization. For non-identical oscillators, synchronization has been established with the help of a generalized method to explain the relationship between the driver and response system. An alternative method is used to produce generalized synchronization (GS) state as a functional relationship between driver-response system. In our work, we have applied an appropriate coupling scheme using OPCL [8,9] method to ensure the generalized synchronization state.

* Corresponding author.
E-mail addresses: ranjit_ism@yahoo.com, ranjit.chaos@gmail.com (R.K. Upadhyay), argham99@gmail.com (A. Mondal), aziz.alaoui@univ-lehavre.fr (M.A. Aziz-Alaoui).

http://dx.doi.org/10.1016/j.apm.2017.02.017
0307-904X/

The theory of synchronization using linear coupling for various coupling strength shows and controls coherent behaviors like complete synchronization (CS) [1,10,11], antiphase synchronization (AS) [12,13], phase synchronization (PS) [14,15], generalized synchronization (GS) [8,16–18], lag synchronization (LS) [19,20], time scale synchronization [21] and so on. To realize CS, the goal dynamics is defined as the product of a constant factor with the driver system i.e., $g(t) = \beta x(t)$. However, the constant, β is considered as the square matrix in the GS regime. To achieve the GS state, the functional relationship, $y(t) = f(x(t))$, between the state variables of the driver ($x \in R^n$) and the response system ($y \in R^n$) was introduced. It can be explained as a state when the response becomes a map of the driver dynamics and the system is $y(t) = Ax(t)$, where A is a transformation matrix. For realizing GS, it is difficult to identify the mathematical structure of the transformation matrix. The GS mechanism ensures more flexibility. Therefore, it can be implemented to realize synchronization in neural computation.

Now, we strive to realize GS between two non-identical coupled neural systems with a reverse engineering method. Neurons are basic function units in nervous system. For signal transformation in neurons, the information is transmitted, encoded and decoded through firing activity of neurons [22]. The electro-physiological research on the Barnacle muscle fiber with applied current [23] show that neuron model could produce complex dynamical behavior [24,25]. Larter et al. [26] proposed a coupled ODE lattice model for the CA3 region of the Hippocampus for the simulation of epileptic seizure. We have considered a 3D modified M-L model system developed by Larter et al. [26]. The model was derived by considering the interactions between the populations of excitatory neurons and inhibitory interneurons and described by the system of nonlinear differential equations [26,27]. Another form of a fast-slow M-L system with bursting phenomenon was proposed by Izhikevich [28]. We consider two non-identical 3D coupled bursting M-L model systems [28,29] to show the GS state for different types of transformation matrices.

A bidirectional coupling function is often found in the neural system while neurons are connected through gap junctions or inhibitory/excitatory synaptic coupling [30–32]. Now, we propose a controller based bidirectional coupling mechanism to show the collective synchronous behavior in a network of four identical H-R neural oscillators [33–37]. We couple the network system by the nonlinear open loop controller (NOLC) [38] coupling method to show the desired complete (CS) and anti-synchronization (AS) behavior. Using the Lyapunov function (LF) stabilty condition, we show the stability of synchronous behavior for this type of bidirectional coupling [38,39]. The difference between the construction of the error systems in the OPCL and NOLC coupling scheme is defined as follows: In the OPCL coupling scheme, the goal dynamics $g(t)$ is the product of linear combination of the system variables of the driver with the transformation matrices whose elements are constants, time dependent state variables of the driver system and the system variables of the H-R dynamical system. However, in the NOLC coupling scheme, the error systems include the linear combinations of the system variables with non-zero constants coefficients. The ratio of the constants are considered as scaling factor which predicts the nature of the synchronization whether it is in CS or AS regimes and reflects the behavior of oscillators size with each other in the network system.

To make our investigations more promising, convincing and sufficient, comparable coupling schemes using bidirectional ring type connections [40–42] have been considered. The desired synchronization has been achieved through Lyapunov stability theory. Our bidirectional coupling scheme presents both CS and AS behavior at appropriate scaling factors. The oscillators can be amplified or attenuated. The method can be extended for a network of N neurons to produce the desired synchronous behavior.

The paper is organized as follows: Section 2 presents the formulation of an OPCL coupling scheme for driver-response system. In Section 3, we introduce the two non-identical 3D modified version of coupled M-L model and coupled bursting M-L model. Then, we describe the coupling method for various types of transformation matrices and produce the GS states with the help of numerical simulations. In Section 4, we present a controller based bidirectional coupling mechanism for a network of four coupled identical H-R neural system to show the collective synchronous behavior. Finally, conclusions are presented in Section 5.

2. Coupling mechanism for generalized synchronization

We first describe the general OPCL [8,9,43] coupling method for a GS state using drive-response unidirectional coupling method in a 3D neural system. We take a dynamical system as a driver

$$\dot{x}(t) = U(x(t)); \quad x(t) \in R^n, \tag{1}$$

and the response system is

$$\dot{y}(t) = V(y(t)); \quad y(t) \in R^n. \tag{2}$$

In the response coupling method, the response oscillator is considered by a desired goal dynamics, $g(t) = \alpha x(t)$, where α is a multiplicative factor [44]. Here, we describe α as a transformation matrix of order $(n \times n)$ by taking the elements (α_{ij}) of the matrix arbitrarily. The elements may contain constants or a function of time or state variables of the driver system and their combinations or state variables of a different dynamical system. We define goal state $g(t) = \alpha x(t)$ in general for a 3D model system as follows:

$$\begin{pmatrix} g_1 \\ g_2 \\ g_3 \end{pmatrix} = \begin{pmatrix} \alpha_{11} & \alpha_{12} & \alpha_{13} \\ \alpha_{21} & \alpha_{22} & \alpha_{23} \\ \alpha_{31} & \alpha_{32} & \alpha_{33} \end{pmatrix} \begin{pmatrix} x_1 \\ x_2 \\ x_3 \end{pmatrix} = \begin{pmatrix} \sum \alpha_{1i} x_i \\ \sum \alpha_{2i} x_i \\ \sum \alpha_{3i} x_i \end{pmatrix}. \tag{3}$$

Therefore, the synchronization scheme is as follows:

$$\begin{cases} \dot{x}(t) = U(x(t)), \\ \dot{y}(t) = V(y(t)) + D(y(t), g(t)), \end{cases} \tag{4}$$

where $D(y(t), g(t))$ is the OPCL coupling term,

$$D(y(t), g(t)) = \dot{g}(t) - V(g(t)) + (H - J(g(t))(y(t) - g(t)). \tag{5}$$

$J(g(t))$ is the *Jacobian* of the function $V(g(t))$ and H is a $(n \times n)$ constant matrix . The error function $e(t) = y(t) - g(t)$ is defined between the trajectories of response system and the goal dynamics. Expanding $V(y) = V(g + e)$ in a Taylor's series expansion we have,

$$V(y) = V(g) + \frac{\partial V(g)}{\partial g} e + \cdots, \tag{6}$$

and we approximate the series at the first order term. With the help of Eqs. (1) and (4)–(6), the error dynamics is given as $\dot{e} = He$. If all the eigenvalues of the H matrix have negative real parts, the error dynamics follow asymptotically stable synchronization ($e \to 0$ as $t \to \infty$), i.e., a targeted GS. To construct the H-matrix, we consider the following procedure: (i) if the element of the *Jacobian* matrix, J_{ij}, is a constant (i.e., the element does not contain any state variable) we refer it as the ijth element of the H-matrix, (ii) otherwise, if J_{ij} contains a state variable, then it is replaced by a constant p_r $(r = 1, 2, 3, \ldots)$ in the H matrix, (iii) the values of the parameters p_r are considered as to satisfy the Routh–Hurwitz (R-H) stability criterion. As a consequence, the choice of the α-matrix does not affect the stability of synchronization. We can change the elements of the transformation matrix without disturbing the synchronization criterion.

In the next section, we describe how to design the coupling mechanism using different types of α-matrices and to implement the desired GS through numerical examples of coupled non-identical neural systems.

3. Numerical examples to show synchronous behavior

In this section, we present various numerical examples to show synchronous behavior. We deal with non-identical coupled modified M-L models, by proposing the coupling to realize the GS state. We considered it for different cases : firstly, in the case for which the elements of transformation matrix as constants. Secondly, the case in which the system (8) plays the role of response system to keep the Hurwitz matrix similar. Then, we use the case for which we take the same systems (7)–(8) however, use the elements of α-matrix as the state variables of the driver system. Finally, we consider the case in which the elements of α-matrix are the state variables of H-R oscillators. Then, we focus on the same question but for two coupled non-identical 3D spiking bursting M-L neural model systems with fast-slow variables to produce synchronous behavior.

3.1. Generalized synchronization for non-identical coupled modified M-L neural model

First, we consider a 3D modified M-L neural system [26,27] and select a transformation matrix that ensures a desired goal dynamics and then propose the coupling to realize the GS state. The variables x_1 and x_3 are mean membrane potentials for excitatory and inhibitory neurons respectively. The variable x_2 represents fraction of open potassium channels at any point of time. The detailed meanings of the parameter values and other details are described in [26,27]. We take several types of transformation matrices for two non-identical coupled neural systems to show GS state. The driver system $\dot{x} = U(x)$ is

$$\begin{pmatrix} \dot{x}_1 \\ \dot{x}_2 \\ \dot{x}_3 \end{pmatrix} = \begin{pmatrix} [-0.5 g_{Ca}\{1 + \tanh((x_1 - V_1)/V_2)\}(x_1 - 1) - g_K x_2 (x_1 - V^K) \\ -g_L(x_1 - V^L) + I - \alpha_{inh} x_3 \{1 + \tanh((x_3 - V_7)/V_6)\}] \\ [\phi \cosh((x_1 - V_3)/2V_4)\{0.5(1 + \tanh((x_1 - V_3)/V_4)) - x_2\}] \\ [bcI + b\alpha_{exc} x_1 \{1 + \tanh((x_1 - V_5)/V_6)\}] \end{pmatrix}, \tag{7}$$

the response system $\dot{y} = V(y)$ is

$$\begin{pmatrix} \dot{y}_1 \\ \dot{y}_2 \\ \dot{y}_3 \end{pmatrix} = \begin{pmatrix} [-0.5 g_{Ca}\{1 + \tanh((y_1 - V_1)/V_2)\}(y_1 - 1) - g_K y_2 (y_1 - V^K) \\ -g'_L(y_1 - V^L) + I - \alpha_{inh} y_3 \{1 + \tanh((y_3 - V_7)/V_6)\}] \\ [\phi' \cosh((y_1 - V_3)/2V_4)\{0.5(1 + \tanh((y_1 - V_3)/V_4)) - y_2\}] \\ [b'c'I + b'\alpha_{exc} y_1 \{1 + \tanh((y_1 - V_5)/V_6)\}] \end{pmatrix}. \tag{8}$$

We consider the parameters of driver and response systems as [26] $g_{Ca} = 1.1, V_1 = -0.01, V_2 = 0.15, g_K = 2, V^K = -0.7, g_L = 0.5, V^L = -0.5, I = 0.3, \alpha_{inh} = 1, \alpha_{exc} = 1, V_7 = 0.0, V_6 = 0.6, \phi = 0.7, V_3 = 0.0, V_4 = 0.3, b = 0.1, c = 0.165, V_5 = 0, g'_L = 1.0, \phi' = 0.4, b' = 0.15, c' = 0.238$. The *Jacobian* of system (8) is

$$J(y)=\begin{pmatrix} a_{11} & a_{12} & a_{13}\\ a_{21} & a_{22} & a_{23}\\ a_{31} & a_{32} & a_{33}\end{pmatrix}, \tag{9}$$

where

$$\begin{aligned}
a_{11} &= -0.5g_{Ca}\{(1+\tanh((y_1-V_1)/V_2))+(1/V_2)(y_1-1)\sec h^2((y_1-V_1)/V_2)\}-g_Ky_2-g'_L,\\
a_{12} &= -g_K(y_1-V^K),\ a_{13}=-\alpha_{inh}\{(1+\tanh((y_3-V_7)/V_6))+(1/V_6)y_3\sec h^2((y_3-V_7)/V_6)\},\\
a_{21} &= 0.5(1/V_4)\phi'\cosh((y_1-V_3)/2V_4)\sec h^2((y_1-V_3)/V_4)\\
&\quad +\phi'(1/2V_4)\sinh((y_1-V_3)/2V_4)\{0.5(1+\tanh((y_1-V_3)/V_4))-y_2\},\\
a_{22} &= -\phi'\cosh((y_1-V_3)/2V_4),\ a_{23}=0,\\
a_{31} &= b'\alpha_{exc}(1+\tanh((y_1-V_5)/V_6))+b'\alpha_{exc}(1/V_6)y_1\sec h^2((y_1-V_5)/V_6),\\
a_{32} &= 0, a_{33}=0.
\end{aligned}$$

We present the H-matrix from the *Jacobian* as

$$H=\begin{pmatrix} p_1 & p_2 & p_3\\ p_4 & p_5 & 0\\ p_6 & 0 & 0\end{pmatrix}. \tag{10}$$

For numerical simulations, we choose the parameter values as $p_1=-2$, $p_2=0$, $p_3=-1$, $p_4=0$, $p_5=-1$, $p_6=1$ so that the H-matrix satisfies R-H criterion. To achieve stable synchronization, we construct the α transformation matrix with an arbitrary choice of elements.

3.1.1. Case I

First, we choose the elements of transformation matrix as constants,

$$\alpha=\begin{pmatrix} 2 & 0 & -1\\ -2 & 0 & 0\\ 2 & -2 & 1\end{pmatrix}. \tag{11}$$

Now, the goal dynamics becomes

$$\begin{pmatrix} g_1\\ g_2\\ g_3\end{pmatrix}=\begin{pmatrix} 2 & 0 & -1\\ -2 & 0 & 0\\ 2 & -2 & 1\end{pmatrix}\begin{pmatrix} x_1\\ x_2\\ x_3\end{pmatrix}=\begin{pmatrix} 2x_1-x_3\\ -2x_1\\ 2x_1-2x_2+x_3\end{pmatrix}, \tag{12}$$

the expression for the coupling term becomes,

$$\begin{aligned}
D &= \begin{pmatrix} 2\dot{x}_1-\dot{x}_3\\ -2\dot{x}_1\\ 2\dot{x}_1-2\dot{x}_2+\dot{x}_3\end{pmatrix}-\begin{pmatrix} [-0.5g_{Ca}\{1+\tanh((g_1-V_1)/V_2)\}(g_1-1)-g_Kg_2(g_1-V^K)\\ -g_L(g_1-V^L)+I-\alpha_{inh}g_3\{1+\tanh((g_3-V_7)/V_6)\}]\\ [\phi\cosh((g_1-V_3)/2V_4)\{0.5(1+\tanh((g_1-V_3)/V_4))-g_2\}]\\ [bcI+b\alpha_{exc}g_1\{1+\tanh((g_1-V_5)/V_6)\}]\end{pmatrix}\\
&\quad +\begin{pmatrix} p_1-a_{11} & p_2-a_{12} & p_3-a_{13}\\ p_4-a_{21} & p_5-a_{22} & 0\\ p_6-a_{31} & 0 & 0\end{pmatrix}\left(\begin{pmatrix} y_1\\ y_2\\ y_3\end{pmatrix}-\begin{pmatrix} g_1\\ g_2\\ g_3\end{pmatrix}\right),
\end{aligned} \tag{13}$$

where

$$\begin{aligned}
a_{11} &= -0.5g_{Ca}\{(1+\tanh((g_1-V_1)/V_2))+(1/V_2)(g_1-1)\sec h^2((g_1-V_1)/V_2)\}-g_Kg_2-g'_L,\\
a_{12} &= -g_K(g_1-V^K),\ a_{13}=-\alpha_{inh}\{(1+\tanh((g_3-V_7)/V_6))+(1/V_6)g_3\sec h^2((g_3-V_7)/V_6)\},\\
a_{21} &= 0.5(1/V_4)\phi'\cosh((g_1-V_3)/2V_4)\sec h^2((g_1-V_3)/V_4)\\
&\quad +\phi'(1/2V_4)\sinh((g_1-V_3)/2V_4)\{0.5(1+\tanh((g_1-V_3)/V_4))-g_2\},\\
a_{22} &= -\phi'\cosh((g_1-V_3)/2V_4),\ a_{23}=0,\\
a_{31} &= b'\alpha_{exc}(1+\tanh((g_1-V_5)/V_6))+b'\alpha_{exc}(1/V_6)g_1\sec h^2((g_1-V_5)/V_6),\\
a_{32} &= 0, a_{33}=0.
\end{aligned} \tag{14}$$

Thus, by adding the coupling term to the RHS of the response system Eq. (8) following the synchronization scheme (4)–(5), it produces the needed response dynamics. It converges to the goal dynamics after the transients die out. The results are graphically presented in Fig. 1. To show the desired GS state, the time series of response variable (y_1) and $(g_1(t))$ are presented in Fig. 1a. The functional relation between the driver and the response system are described in terms of goal dynamics, $g_1=\sum_{i=1,2,3}\alpha_{1i}x_i=2x_1-x_3$. This shows 1:1 correlation to ensure the GS (Fig. 1b). The response variables (y_2) and (y_3) follow similar type GS relations with goal dynamics which has been presented in Fig. 1c and d. The time series of

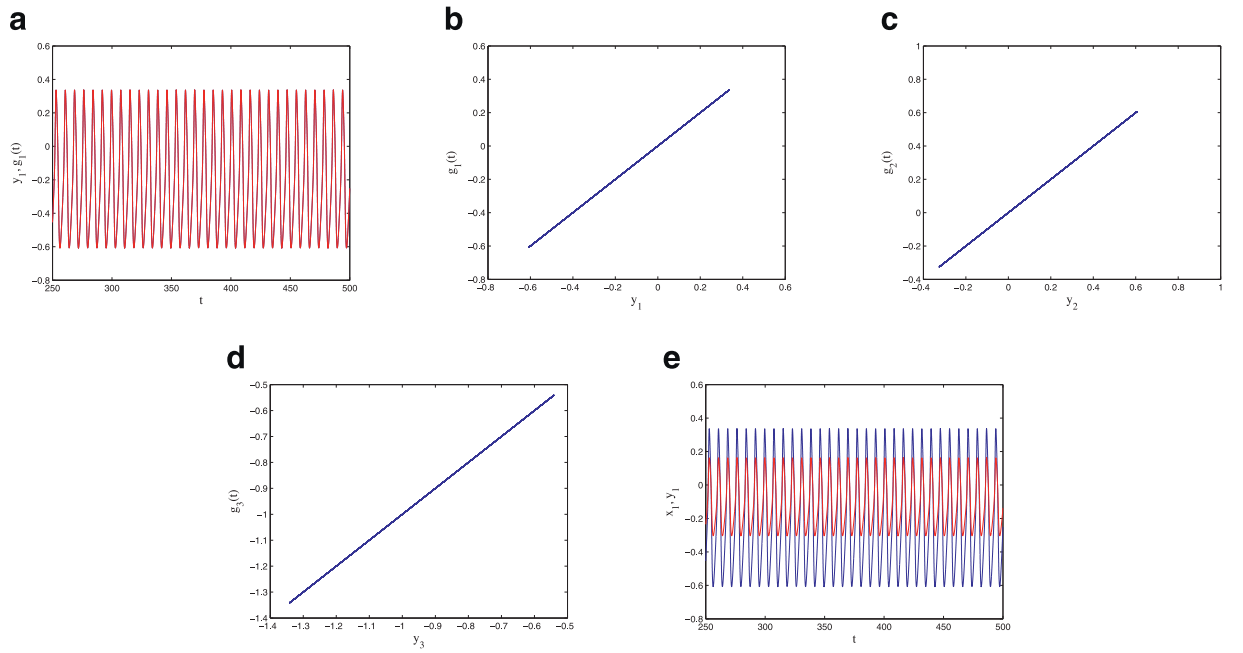

Fig. 1. GS in non-identical coupled modified M-L neural system defined by a constant matrix: (*a*) time series of y_1 and g_1; (*b*) g_1 against y_1; (*c*) g_2 against y_2; (*d*) g_3 against y_3 confirm GS relation. (*e*) time series of x_1 and y_1.

the response (y_1) with the driver (x_1) show identical synchronization but it may have PS. In reality, to establish a GS state, we follow a simple technique that satisfy 1:1 correlation between the response and the transformed driver states.

3.1.2. Case II

Next, we consider system (8) as the response system and hence the Hurwitz matrix remains same. We use systems (7) and (8) and change the elements of the α-transformation matrix as periodic functions

$$\alpha = \begin{pmatrix} 2\sin(0.5t) & 0 & 0 \\ 0 & 0.5\cos(-0.8t) & 0 \\ 0 & 0 & 1 \end{pmatrix}. \tag{15}$$

Now, the goal dynamics becomes

$$\begin{pmatrix} g_1 \\ g_2 \\ g_3 \end{pmatrix} = \begin{pmatrix} 2\sin(0.5t) & 0 & 0 \\ 0 & 0.5\cos(-0.8t) & 0 \\ 0 & 0 & 1 \end{pmatrix} \begin{pmatrix} x_1 \\ x_2 \\ x_3 \end{pmatrix} = \begin{pmatrix} 2\sin(0.5t)x_1 \\ 0.5\cos(-0.8t)x_2 \\ x_3 \end{pmatrix}, \tag{16}$$

and the expression of the coupler becomes

$$\begin{aligned} D = & \begin{pmatrix} 2\sin(0.5t)\dot{x}_1 + \cos(0.5t)x_1 \\ 0.5\cos(-0.8t)\dot{x}_2 + 0.4\sin(-0.8t)x_2 \\ \dot{x}_3 \end{pmatrix} \\ & - \begin{pmatrix} [-0.5g_{Ca}\{1+\tanh((g_1-V_1)/V_2)\}(g_1-1) - g_K g_2(g_1-V^K) \\ -g_L(g_1-V^L) + I - \alpha_{inh}g_3\{1+\tanh((g_3-V_7)/V_6)\}] \\ [\phi\cosh((g_1-V_3)/2V_4)\{0.5(1+\tanh((g_1-V_3)/V_4)) - g_2\}] \\ [bcI + b\alpha_{exc}g_1\{1+\tanh((g_1-V_5)/V_6)\}] \end{pmatrix} \\ & + \begin{pmatrix} p_1-a_{11} & p_2-a_{12} & p_3-a_{13} \\ p_4-a_{21} & p_5-a_{22} & 0 \\ p_6-a_{31} & 0 & 0 \end{pmatrix} \left(\begin{pmatrix} y_1 \\ y_2 \\ y_3 \end{pmatrix} - \begin{pmatrix} g_1 \\ g_2 \\ g_3 \end{pmatrix} \right). \end{aligned} \tag{17}$$

where the expressions a_{11}, a_{12}, a_{13}, a_{21}, a_{22} and a_{31} are same as described in Eq. (14). Arbitrarily, we have taken periodic functions in Eq. (15) without disturbing the stability of synchronization. Fig. 2a shows the time series of response variable (y_1) and the goal dynamics (g_1). Figs. 2b–d indicates GS. The time series of system variables x_1 and y_1 are plotted in

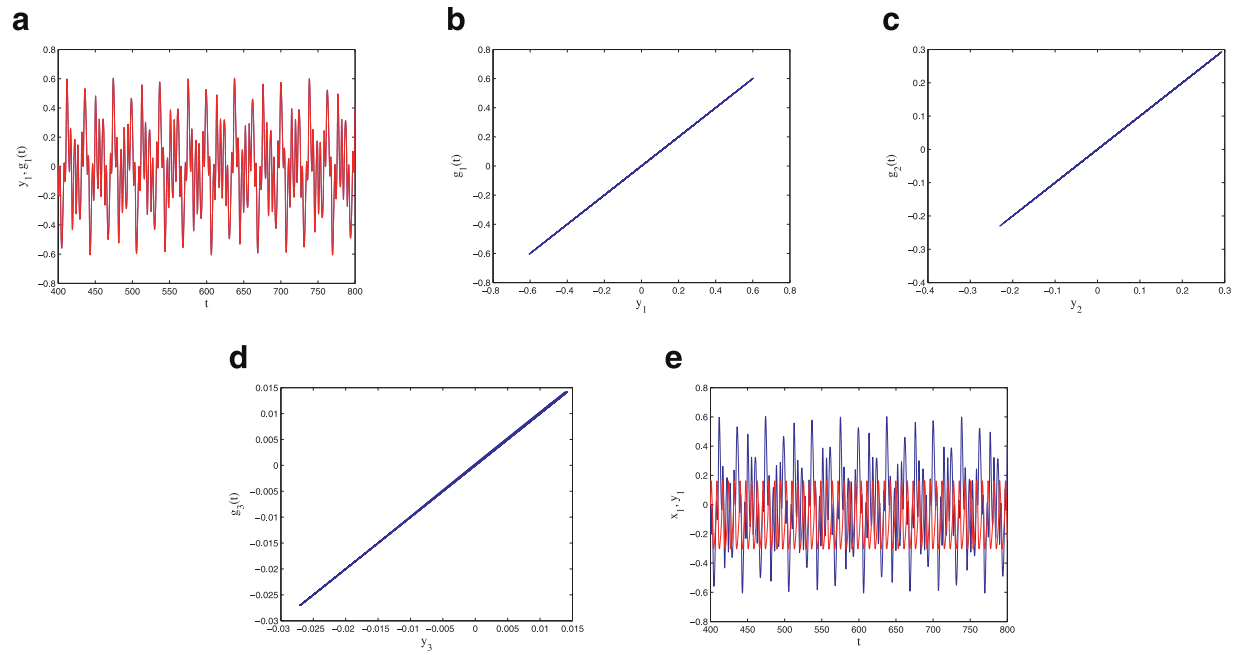

Fig. 2. GS in non-identical coupled modified M-L neural system defined by α-matrix with periodic functions: (a) time series of y_1 and g_1; (b) g_1 against response variable y_1; (c) g_2 against y_2; (d) g_3 against y_3 confirm GS relation. (e) time series of x_1 and y_1.

Fig. 2e appears to be in PS state. However, the α-matrix has the time dependent functions, it does not affect the stability of synchronization as mentioned in Section 2.

3.1.3. Case III

Next, we take the same systems (7) and (8) but use the elements of α-matrix as the state variables of the driver system,

$$\alpha = \begin{pmatrix} x_1 & x_2 & 0 \\ x_2 & x_1 & 0 \\ 0 & 0 & 1 \end{pmatrix}. \tag{18}$$

Choosing this type of α-matrix which has the high degree of nonlinearity in goal state. Now, the goal dynamics becomes

$$\begin{pmatrix} g_1 \\ g_2 \\ g_3 \end{pmatrix} = \begin{pmatrix} x_1 & x_2 & 0 \\ x_2 & x_1 & 0 \\ 0 & 0 & 1 \end{pmatrix} \begin{pmatrix} x_1 \\ x_2 \\ x_3 \end{pmatrix} = \begin{pmatrix} {x_1}^2 + {x_2}^2 \\ 2x_1x_2 \\ x_3 \end{pmatrix}, \tag{19}$$

and the coupling term becomes

$$D = \begin{pmatrix} 2x_1\dot{x}_1 + 2x_2\dot{x}_2 \\ 2(x_1\dot{x}_2 + x_2\dot{x}_1) \\ \dot{x}_3 \end{pmatrix} - \begin{pmatrix} [-0.5g_{Ca}\{1 + \tanh((g_1 - V_1)/V_2)\}(g_1 - 1) - g_K g_2(g_1 - V^K) \\ -g_L(g_1 - V^L) + I - \alpha_{inh}g_3\{1 + \tanh((g_3 - V_7)/V_6)\}] \\ [\phi \cosh((g_1 - V_3)/2V_4)\{0.5(1 + \tanh((g_1 - V_3)/V_4)) - g_2\}] \\ [bcI + b\alpha_{exc}g_1\{1 + \tanh((g_1 - V_5)/V_6)\}] \end{pmatrix}$$
$$+ \begin{pmatrix} p_1 - a_{11} & p_2 - a_{12} & p_3 - a_{13} \\ p_4 - a_{21} & p_5 - a_{22} & 0 \\ p_6 - a_{31} & 0 & 0 \end{pmatrix} \left(\begin{pmatrix} y_1 \\ y_2 \\ y_3 \end{pmatrix} - \begin{pmatrix} g_1 \\ g_2 \\ g_3 \end{pmatrix} \right), \tag{20}$$

where the expressions a_{11}, a_{12}, a_{13}, a_{21}, a_{22} and a_{31} are same as described in Eq. (14). Numerical simulation results are plotted in Fig. 3. The time series of the response variable y_1 and g_1 is plotted in Fig. 3a. The time series plot of x_1 and y_1 given in Fig. 3e apparently shows that there phases are same. This occurs for nonlinearity terms in the α-matrix. However, the plots y_1 vs g_1, y_2 vs g_2 and y_3 vs g_3 are presented in Fig. 3b–d and ensures GS between driver and response systems.

3.1.4. Case IV

Now, we consider the idea of GS process using the elements of α-matrix as the state variables of Hindmarsh–Rose (H-R) neural oscillatory system [34,35,37], while the driver and response systems are non-identical as given in (7) and (8). We

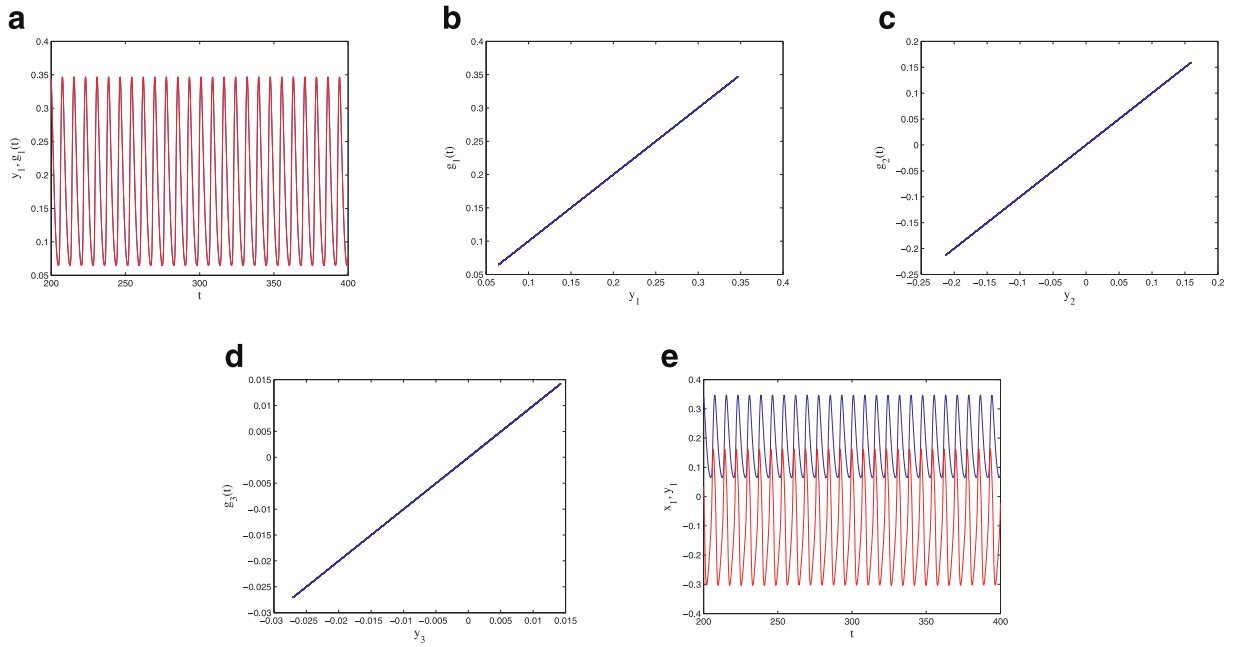

Fig. 3. GS in non-identical coupled modified M-L neural system defined by α-matrix with elements of driver variables: (a) time series of y_1 and g_1; (b) g_1 against response variable y_1; (c) g_2 against y_2; (d) g_3 against y_3 show CS. (e) time series of x_1 and y_1.

write the dynamics of the H-R model as

$$\begin{cases} u_1 = u_2 - u_1^3 + au_1^2 - u_3 + I, \\ u_2 = 1 - 5u_1^2 - u_2, \\ u_3 = cd(u_1 + 1.6) - cu_3, \end{cases} \tag{21}$$

where the value of the parameters are taken as $a = 3, I = 4.1, c = 0.003, d = 5$. The α-matrix is in the form

$$\alpha = \begin{pmatrix} u_1 & u_2 & 0 \\ u_2 & u_1 & 0 \\ 0 & 0 & 1 \end{pmatrix}, \tag{22}$$

the goal dynamics is

$$\begin{pmatrix} g_1 \\ g_2 \\ g_3 \end{pmatrix} = \begin{pmatrix} u_1 & u_2 & 0 \\ u_2 & u_1 & 0 \\ 0 & 0 & 1 \end{pmatrix} \begin{pmatrix} x_1 \\ x_2 \\ x_3 \end{pmatrix} = \begin{pmatrix} u_1x_1 + u_2x_2 \\ u_2x_1 + u_1x_2 \\ x_3 \end{pmatrix}. \tag{23}$$

The coupler becomes

$$D = \begin{pmatrix} \dot{u}_1x_1 + u_1\dot{x}_1 + \dot{u}_2x_2 + u_2\dot{x}_2 \\ \dot{u}_2x_1 + u_2\dot{x}_1 + \dot{u}_1x_2 + u_1\dot{x}_2 \\ \dot{x}_3 \end{pmatrix} - \begin{pmatrix} [-0.5g_{Ca}\{1 + \tanh((g_1 - V_1)/V_2)\}(g_1 - 1) - g_Kg_2(g_1 - V^K) \\ -g_L(g_1 - V^L) + I - \alpha_{inh}g_3\{1 + \tanh((g_3 - V_7)/V_6)\}] \\ [\phi\cosh((g_1 - V_3)/2V_4)\{0.5(1 + \tanh((g_1 - V_3)/V_4)) - g_2\}] \\ [bcI + b\alpha_{exc}g_1\{1 + \tanh((g_1 - V_5)/V_6)\}] \end{pmatrix}$$
$$+ \begin{pmatrix} p_1 - a_{11} & p_2 - a_{12} & p_3 - a_{13} \\ p_4 - a_{21} & p_5 - a_{22} & 0 \\ p_6 - a_{31} & 0 & 0 \end{pmatrix} \left(\begin{pmatrix} y_1 \\ y_2 \\ y_3 \end{pmatrix} - \begin{pmatrix} g_1 \\ g_2 \\ g_3 \end{pmatrix} \right), \tag{24}$$

where the expressions a_{11}, a_{12}, a_{13}, a_{21}, a_{22} and a_{31} are same as described in Eq. (14). The OPCL coupling method appropriately works to realize the GS between the driver and response systems as described in Fig. 4. It is not only restricted to modified M-L system and H-R system but it also works for other combinations of driver-response systems under suitable conditions to produce desired GS state without disturbing stability of synchronization. Similarly, as the previous cases the GS relation is established shown in Fig. 4a–d.

3.2. Generalized synchronization for non-identical coupled spiking bursting M-L neural model

Now, we investigate two coupled non-identical 3D spiking bursting coupled M-L neural model systems with fast-slow variables [28,29] to produce synchronous behavior. The first two variables x_1 and x_2 represent fast process associated with

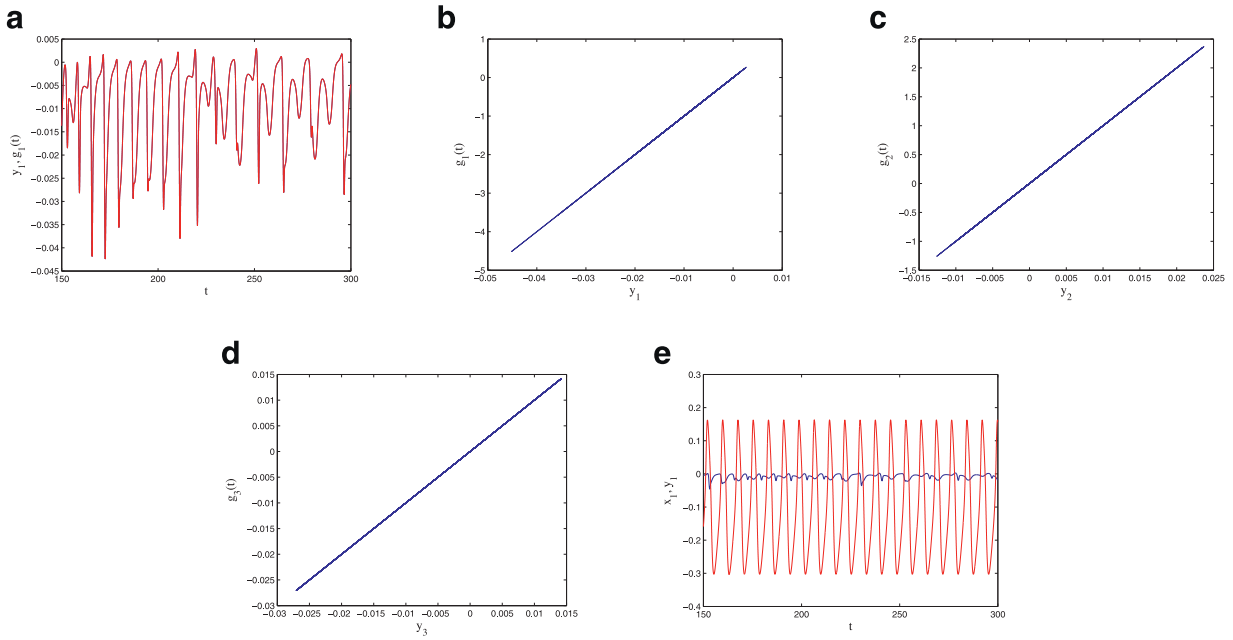

Fig. 4. GS in non-identical coupled modified M-L neural system defined by α-matrix with elements consisting of state variables of H-R system: (a) time series of y_1 and g_1; (b) g_1 against response variable y_1; (c) g_2 against y_2; (d) g_3 against y_3 show GS; (e) time series of x_1 and y_1 show no correlation.

spiking behavior and the third variable x_3 describes relatively slow process that modulates fast spiking. The small parameter $0 < \varepsilon \ll 1$ represents the ratio of time scale between spiking and modulation. Different types of bursting are usually exhibited by the activity of slow parameter x_3. The value of equilibrium potentials of the ion channel V^{Ca} has been taken as one [28,29,45]. The neural model system is said $(m+k)$ dimensional, where the fast subsystem is m-dimensional and the slow subsystem is k-dimensional i.e., it is a $(2+1)$ dimensional neural system. The driver $\dot{x} = U(x)$ is

$$\begin{pmatrix} \dot{x}_1 \\ \dot{x}_2 \\ \dot{x}_3 \end{pmatrix} = \begin{pmatrix} [0.5g_{Ca}\{1+\tanh((x_1-V_1)/V_2)\}(1-x_1) + g_K x_2(V^K - x_1) + g_L(V^L - x_1) + x_3] \\ [\phi\cosh((x_1-V_3)/2V_4)\{0.5(1+\tanh((x_1-V_3)/V_4)) - x_2\}] \\ -\varepsilon(V_0 + x_1) \end{pmatrix}, \tag{25}$$

the response system is $\dot{y} = V(y)$ is

$$\begin{pmatrix} \dot{y}_1 \\ \dot{y}_2 \\ \dot{y}_3 \end{pmatrix} = \begin{pmatrix} [0.5g_{Ca}\{1+\tanh((y_1-V_1)/V_2)\}(1-y_1) + g_K y_2(V^{K'} - y_1) + g_L(V^L - y_1) + y_3] \\ [\phi\cosh((y_1-V_3)/2V_4)\{0.5(1+\tanh((y_1-V_3)/V_4)) - y_2\}] \\ -\varepsilon'(V_0 + y_1) \end{pmatrix}. \tag{26}$$

We consider the parameters of driver and response system as [28] $g_{Ca} = 1.2, V_1 = -0.01, V_2 = 0.15, g_K = 2, V^K = -0.7, g_L = 0.5, V^L = -0.5, \phi = 1/3, V_3 = 0.1, V_4 = 0.05, V_0 = 0.2, V^{K'} = -1.3, \varepsilon = 0.005, \varepsilon' = 0.003$. The *Jacobian* of the response system (26) is

$$J = \begin{pmatrix} a_{11} & a_{12} & a_{13} \\ a_{21} & a_{22} & a_{23} \\ a_{31} & a_{32} & a_{33} \end{pmatrix}, \tag{27}$$

where

$$\begin{aligned} a_{11} &= 0.5g_{Ca}\{-(1+\tanh((g_1-V_1)/V_2)) + (1/V_2)(1-g_1)\,\mathrm{sec}\,h^2((g_1-V_1)/V_2)\} - g_K g_2 - g_L, \\ a_{12} &= g_K(V^{K'} - g_1),\ a_{13} = 1, \\ a_{21} &= 0.5(1/V_4)\phi\cosh((g_1-V_3)/2V_4)\,\mathrm{sec}\,h^2((g_1-V_3)/V_4) \\ &\quad + \phi(1/2V_4)sinh((g_1-V_3)/2V_4)\{0.5(1+\tanh((g_1-V_3)/V_4)) - g_2\}, \\ a_{22} &= -\phi'\cosh((g_1-V_3)/2V_4),\ a_{23} = 0, \\ a_{31} &= -\varepsilon', \\ a_{32} &= 0, a_{33} = 0. \end{aligned} \tag{28}$$

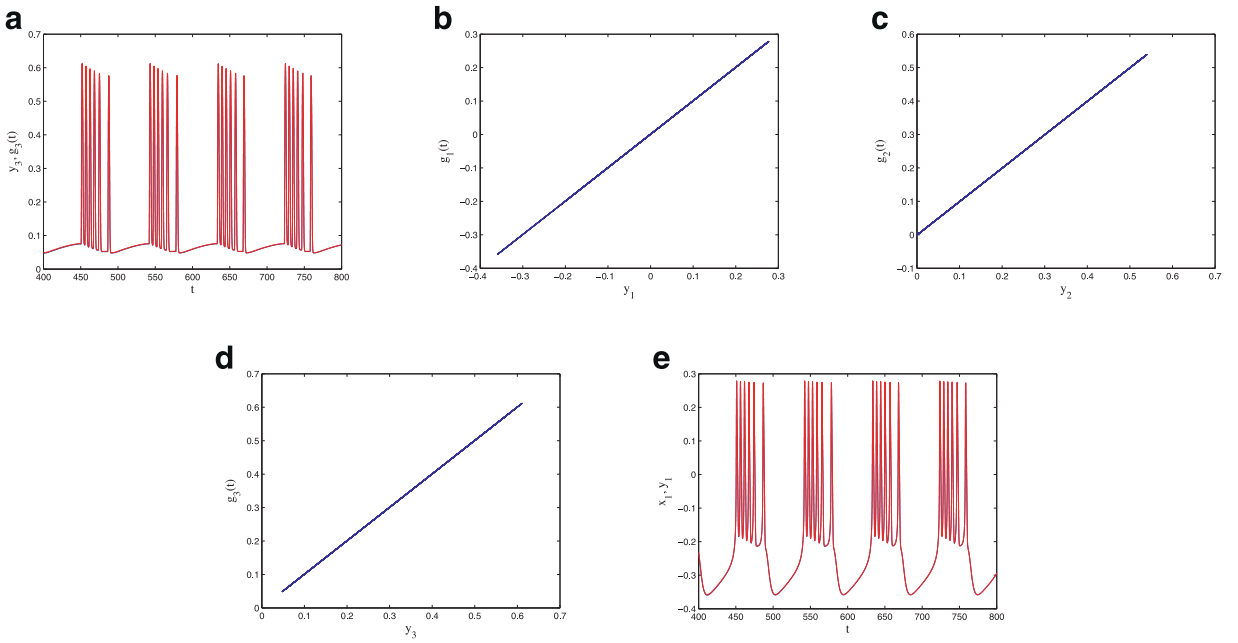

Fig. 5. GS in coupled non-identical spiking bursting M-L neural system with fast-slow variables defined by a constant matrix: (*a*) time series of y_3 and g_3; (*b*) g_1 against y_1; (*c*) g_2 against y_2; (*d*) g_3 against y_3 confirm GS relation. (*e*) time series of x_1 and y_1.

We write the H-matrix from the *Jacobian* as described above in Eq. (27) as

$$H = \begin{pmatrix} p_1 & p_2 & 1 \\ p_3 & p_4 & 0 \\ -\varepsilon' & 0 & 0 \end{pmatrix}. \tag{29}$$

For numerical calculation, we set the value of parameters as $p_1 = 0, p_2 = 1, p_3 = -1$ and $p_4 = -1$ which satisfy the R-H criterion of the H-matrix.

3.2.1. Case I

First, we select an arbitrary choice of the elements of the α-transformation matrix as constants

$$\alpha = \begin{pmatrix} 1 & 0 & 0 \\ 0 & 1 & 0 \\ 0 & 1 & 1 \end{pmatrix}, \tag{30}$$

when the goal dynamics becomes

$$\begin{pmatrix} g_1 \\ g_2 \\ g_3 \end{pmatrix} = \begin{pmatrix} 1 & 0 & 0 \\ 0 & 1 & 0 \\ 0 & 1 & 1 \end{pmatrix} \begin{pmatrix} x_1 \\ x_2 \\ x_3 \end{pmatrix} = \begin{pmatrix} x_1 \\ x_2 \\ x_2 + x_3 \end{pmatrix}. \tag{31}$$

Now, the coupling term becomes

$$D = \begin{pmatrix} \dot{x}_1 \\ \dot{x}_2 \\ \dot{x}_2 + \dot{x}_3 \end{pmatrix} - \begin{pmatrix} [0.5 g_{Ca}\{1 + \tanh((g_1 - V_1)/V_2)\}(1 - g_1) + g_K g_2 (V^{K'} - g_1) + g_L (V^L - g_1) + g_3] \\ [\phi \cosh((g_1 - V_3)/2V_4)\{0.5(1 + \tanh((g_1 - V_3)/V_4)) - g_2\}] \\ -\varepsilon'(V_0 + g_1) \end{pmatrix} + \begin{pmatrix} p_1 - a_{11} & p_2 - a_{12} & 0 \\ p_3 - a_{21} & p_4 - a_{22} & 0 \\ 0 & 0 & 0 \end{pmatrix} \left(\begin{pmatrix} y_1 \\ y_2 \\ y_3 \end{pmatrix} - \begin{pmatrix} g_1 \\ g_2 \\ g_3 \end{pmatrix} \right), \tag{32}$$

where the values of a_{11}, a_{12}, a_{21}, a_{22} are described in Eq. (28). Next, we add the coupling term (Eq. (32)) to the RHS of Eq. (26) to produce the response dynamics. It converges to the desired goal dynamics after the transients part. Numerical results are shown in Fig. 5. Time series plot of y_3 and g_3 are shown in Fig. 5a. The GS relation is confirmed which is shown in Fig. 5b–d and plotted between $g_1(t)$ vs $y_1(t)$, $g_2(t)$ vs $y_2(t)$ and $g_3(t)$ vs $y_3(t)$ respectively. The time series of driver x_1 and response y_1 has been plotted in Fig. 5e.

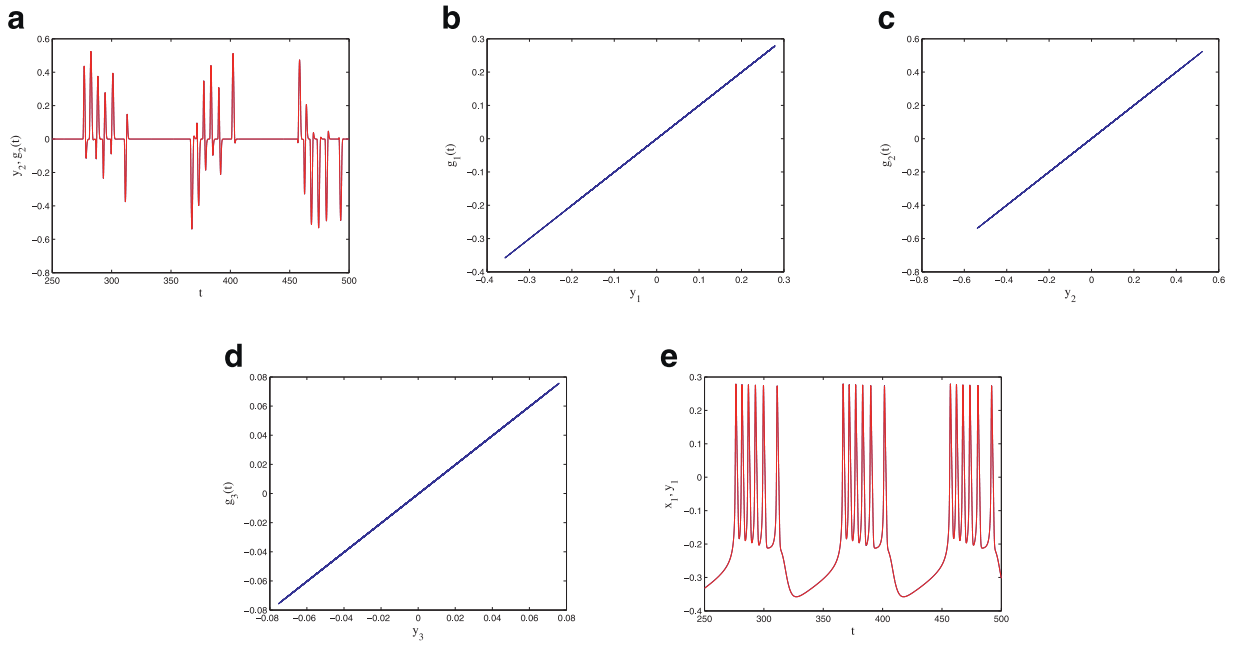

Fig. 6. GS in non-identical coupled spiking bursting M-L neural system defined by α-matrix with periodic functions: (a) time series of y_2 and g_2; (b) g_1 against response variable y_1; (c) g_2 against y_2; (d) g_3 against y_3 confirm GS relation. (e) time series of x_1 and y_1 respectively.

3.2.2. Case II

Next, we take the systems (25) and (26) as the driver-response system and the Hurwitz matrix remains unchanged. We select the elements of the α-matrix as periodic functions

$$\alpha = \begin{pmatrix} 1 & 0 & 0 \\ 0 & \cos t & 0 \\ 0 & 0 & \sin t \end{pmatrix}, \tag{33}$$

while the goal dynamics becomes

$$\begin{pmatrix} g_1 \\ g_2 \\ g_3 \end{pmatrix} = \begin{pmatrix} 1 & 0 & 0 \\ 0 & \cos t & 0 \\ 0 & 0 & \sin t \end{pmatrix} \begin{pmatrix} x_1 \\ x_2 \\ x_3 \end{pmatrix} = \begin{pmatrix} x_1 \\ x_2 \cos t \\ x_3 \sin t \end{pmatrix}, \tag{34}$$

and the coupling term is

$$D = \begin{pmatrix} \dot{x}_1 \\ \dot{x}_2 \cos t - x_2 \sin t \\ \dot{x}_3 \sin t + x_3 \cos t \end{pmatrix} - \begin{pmatrix} [0.5 g_{Ca}\{1 + \tanh((g_1 - V_1)/V_2)\}(1 - g_1) + g_K g_2 (V^{K'} - g_1) + g_L (V^L - g_1) + g_3] \\ [\phi \cosh((g_1 - V_3)/2V_4)\{0.5(1 + \tanh((g_1 - V_3)/V_4)) - g_2\}] \\ -\varepsilon'(V_0 + g_1) \end{pmatrix} + \begin{pmatrix} p_1 - a_{11} & p_2 - a_{12} & 0 \\ p_3 - a_{21} & p_4 - a_{22} & 0 \\ 0 & 0 & 0 \end{pmatrix} \left(\begin{pmatrix} y_1 \\ y_2 \\ y_3 \end{pmatrix} - \begin{pmatrix} g_1 \\ g_2 \\ g_3 \end{pmatrix} \right). \tag{35}$$

We arbitrarily select the elements of α-matrix as the periodic functions in Eq. (33). The values of a_{11}, a_{12}, a_{21}, a_{22} are explained in Eq. (28). We can choose other functions without disturbing the stability of synchronization. The simulated graphical results are shown in Fig. 6. The synchronization has been established though the α-matrix is chosen as periodic functions.

3.2.3. Case III

In next example, we use the same systems (25) and (26) but the α-matrix contains the state variable of driver system,

$$\alpha = \begin{pmatrix} x_1 & x_2 & 0 \\ x_2 & x_1 & 0 \\ 0 & 0 & 1 \end{pmatrix}. \tag{36}$$

This type of matrix upraises the degree of nonlinearity in the goal dynamics. Now, the goal dynamics is

$$\begin{pmatrix} g_1 \\ g_2 \\ g_3 \end{pmatrix} = \begin{pmatrix} x_1 & x_2 & 0 \\ x_2 & x_1 & 0 \\ 0 & 0 & 1 \end{pmatrix} \begin{pmatrix} x_1 \\ x_2 \\ x_3 \end{pmatrix} = \begin{pmatrix} x_1^2 + x_2^2 \\ 2x_1 x_2 \\ x_3 \end{pmatrix}, \tag{37}$$

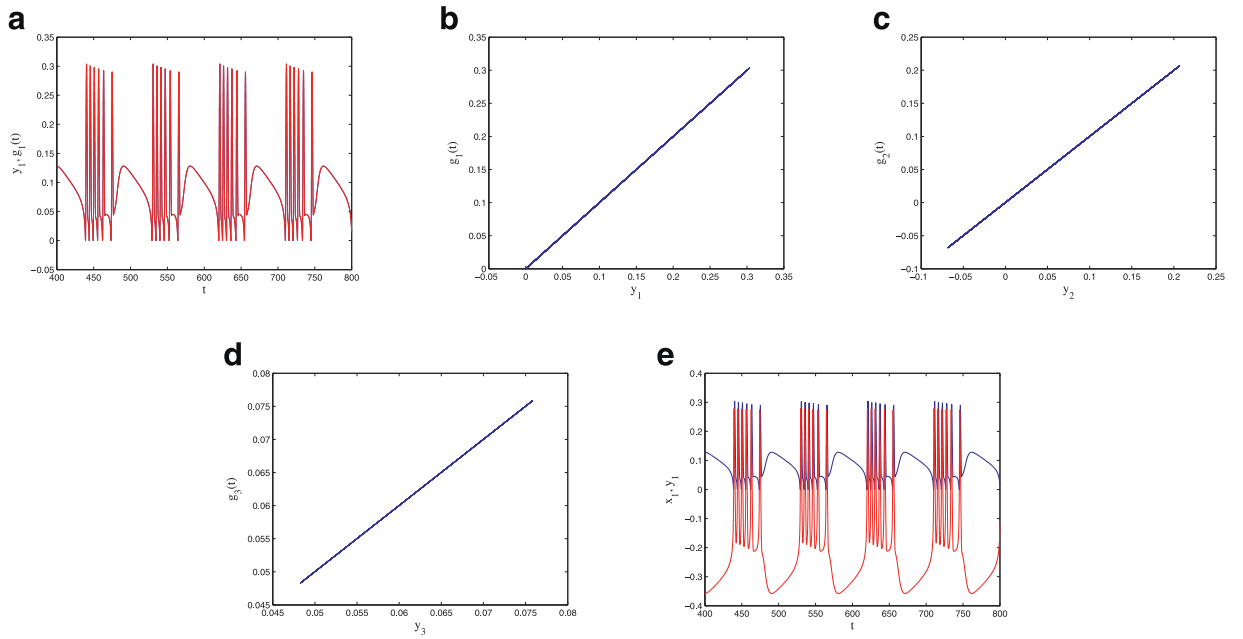

Fig. 7. GS in non-identical coupled spiking bursting M-L neural system defined by α-matrix with periodic functions: (*a*) time series of y_1 and g_1; (*b*) g_1 against y_1; (*c*) g_2 against y_2; (*d*) g_3 against y_3 confirm GS relation. (*e*) time series of x_1 and y_1.

and the coupling term is

$$D = \begin{pmatrix} 2(x_1\dot{x}_1 + x_2\dot{x}_2) \\ 2(x_1\dot{x}_2 + \dot{x}_1x_2) \\ \dot{x}_3 \end{pmatrix} - \begin{pmatrix} [g_{Ca}0.5\{1+\tanh((g_1-V_1)/V_2)\}(1-g_1) + g_Kg_2(V^{K'}-g_1) \\ +g_L(V^L-g_1)+g_3] \\ [\phi\cosh((g_1-V_3)/2V_4)\{0.5(1+\tanh((g_1-V_3)/V_4))-g_2\}] \\ -\varepsilon'(V_0+g_1) \end{pmatrix} + \begin{pmatrix} p_1-a_{11} & p_2-a_{12} & 0 \\ p_3-a_{21} & p_4-a_{22} & 0 \\ 0 & 0 & 0 \end{pmatrix} \left(\begin{pmatrix} y_1 \\ y_2 \\ y_3 \end{pmatrix} - \begin{pmatrix} g_1 \\ g_2 \\ g_3 \end{pmatrix} \right) \left(\begin{pmatrix} y_1 \\ y_2 \\ y_3 \end{pmatrix} - \begin{pmatrix} g_1 \\ g_2 \\ g_3 \end{pmatrix} \right). \tag{38}$$

The values of a_{11}, a_{12}, a_{21}, a_{22} are described in Eq. (28). The numerical results are shown in Fig. 7 which shows that the targeted GS relation is obtained using the proposed OPCL coupling scheme. The time series of x_1 and y_1 apparently shows that it may follow anti synchronous behavior. In reality, the GS relation is confirmed by the 1:1 correlation between the driver and the response variables.

3.2.4. Case IV

Finally, we present the same systems (25) and (26) as driver and response systems but we change the elements of α-matrix as the state variable of H-R system Eq. (21) and the α-matrix is taken as

$$\alpha = \begin{pmatrix} 0.01u_1 & 0.01u_2 & 0 \\ 0.01u_2 & 0.01u_1 & 0 \\ 0 & 0 & 1 \end{pmatrix}. \tag{39}$$

The goal dynamics becomes

$$\begin{pmatrix} g_1 \\ g_2 \\ g_3 \end{pmatrix} = \begin{pmatrix} 0.01u_1 & 0.01u_2 & 0 \\ 0.01u_2 & 0.01u_1 & 0 \\ 0 & 0 & 1 \end{pmatrix} \begin{pmatrix} x_1 \\ x_2 \\ x_3 \end{pmatrix} = \begin{pmatrix} 0.01u_1x_1 + 0.01u_2x_2 \\ 0.01u_2x_1 + 0.01u_1x_2 \\ x_3 \end{pmatrix}, \tag{40}$$

and the coupler is

$$D = \begin{pmatrix} 0.01(\dot{u}_1x_1 + u_1\dot{x}_1) + 0.01(\dot{u}_2x_2 + u_2\dot{x}_2) \\ 0.01(\dot{u}_2x_1 + u_2\dot{x}_1) + 0.01(\dot{u}_1x_2 + u_1\dot{x}_2) \\ \dot{x}_3 \end{pmatrix}$$

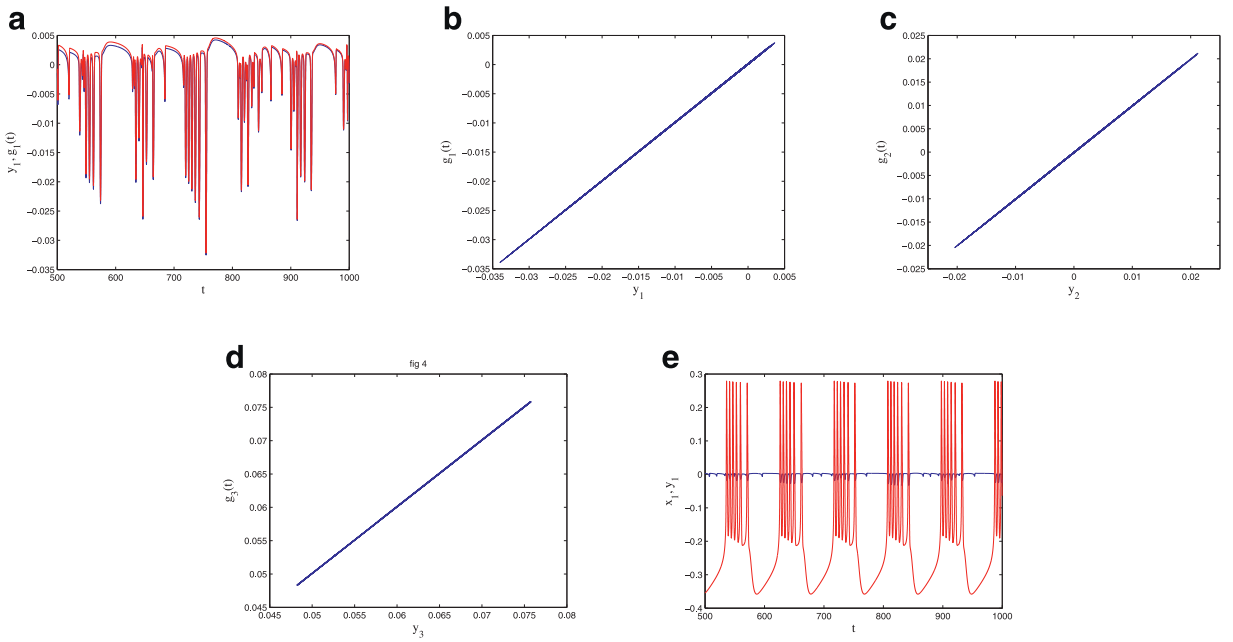

Fig. 8. GS in non-identical coupled spiking bursting M-L neural system defined by α-matrix with elements consisting of state variables of Hindmarsh–Rose system: (a) time series of y_1 and g_1; (b) g_1 against response variable y_1; (c) g_2 against y_2; (d) g_3 against y_3 confirm GS relation and (a) time series of x_1 and y_1.

$$-\begin{pmatrix} [g_{Ca}0.5\{1+\tanh((g_1-V_1)/V_2)\}(1-g_1)+g_Kg_2(V^{K'}-g_1)+g_L(V^L-g_1)+g_3] \\ [\phi\cosh((g_1-V_3)/2V_4)\{0.5(1+\tanh((g_1-V_3)/V_4))-g_2\}] \\ -\varepsilon'(V_0+g_1) \end{pmatrix}$$
$$+\begin{pmatrix} p_1-a_{11} & p_2-a_{12} & 0 \\ p_3-a_{21} & p_4-a_{22} & 0 \\ 0 & 0 & 0 \end{pmatrix}\left(\begin{pmatrix} y_1 \\ y_2 \\ y_3 \end{pmatrix}-\begin{pmatrix} g_1 \\ g_2 \\ g_3 \end{pmatrix}\right). \tag{41}$$

The numerical results are presented in Fig. 8. The simulated time series of the driver and response variables demonstrates no correlation. However, due to the higher nonlinearity of the α transformation matrix, the targeted GS is properly working using the OPCL method. The simulated time series of y_1 and g_1 is presented in Fig. 8a. The time series between driver (x_1) and the response (y_1) states does not indicate any correlation. However, the OPCL coupling method establishes a GS relation in driver-response neural systems followed from 1:1 correlation presented in Fig 8b–d. It works properly in realizing functional relation when the elements of α-matrix are chosen from other dynamical system. We have a freedom in applying this method for choosing positive as well as negative values for the elements of constant α transformation ($n \times n$) matrix and we can choose the proper coupling term to control response oscillating neural system without affecting the stability of synchronization.

4. Synchronization of coupled network of Hindmarsh–Rose neural oscillators

In this section, we construct and apply a NOLC based bidirectional coupling mechanism to a network of four H-R oscillators to show CS and AS states in different cases. We also consider a comparable method to a network of H-R oscillators using a bidirectional ring type connection. Finally, a Lyapunov direct method has been applied to establish the desired synchronization state.

The spiking bursting dynamical behavior of the well known Hindmarsh–Rose (H-R) [33,34,36,37] neural model is well studied in neural computation and the nature of generation of action potential depends on some control parameters. The model is the modified version of the Fitzhugh–Nagumo neural model [46]. It was originally constructed to model the synchronous behavior of firing of two snail neurons. By fixing some parameters, the model reads as follows:

$$\begin{aligned} \dot{x}(t) &= y(t) - x^3(t) + 3x^2(t) - z(t) + I, \\ \dot{y}(t) &= 1 - 5x^2(t) - y(t), \\ \dot{z}(t) &= rs(x(t) + 1.6) - rz(t), \end{aligned} \tag{42}$$

where $x(t)$ represents the membrane potential of the neuronal cell, the recovery variables $y(t)$ and $z(t)$ which take into account transport of ions through ion channels across the membrane. The spiking variable $y(t)$ measures the rate of sodium

and potassium ion transport through fast ion channels. The bursting variable $z(t)$ measures the rate of other ions transport through slow ion channels. The parameter value r represents difference scale between fast and slow recovery variables. I is the applied current enter into the neuron. $z(t)$ is the slow dynamical variable and depends on the parameter value $r(0 < r \ll 1)$ which is very small and performs the bursting behavior and s performs the adaptation behavior of the H-R model [35,37]. Bursting behavior is a multi-scale type phenomenon where spiking or bursting or both can occur. To show the examples of real world applications in biological oscillating systems, we take various parameter sets such as (i) $I = 3.3, r = 0.001, s = 4$, (ii) $I = 1.345, r = 0.001, s = 4$ and (iii) $I = 3.05, r = 0.005, s = 4$ for computation at which the system exhibits spiking, periodic bursting and chaotic bursting behavior respectively which is often found in neural system [31,35,37,40].

We apply a NOLC based bidirectional coupling mechanism [38,39] to a network of 4-oscillators to show CS and AS states. We present the formulation of coupling method for N oscillating systems as follows:

$$\dot{w}_i = f(w_i) + W_{w_i}, \qquad i = 1,\ 2,\ 3, \ldots, N, \tag{43}$$

where $w_i = (x_i,\ y_i,\ z_i)^T$ is the state variables vector and $f(w_i) \in R^n$ represents the flow of the ith system for uncoupled condition. W_{w_i} is the controller that confirms the coupling between the ith and the remaining oscillators in the network system. The bidirectional coupling procedure is calculated for the network of N H-R oscillators using the LF stability and various non-zero values of scaling factors. The error function for a network of N oscillators is defined as [39]

$$e_{x_j} = (N-1)x_N - \alpha_N \sum_{i=1}^{N-1} x_i/\alpha_i, \tag{44}$$

similarly, e_{y_j} and e_{z_j} are defined as above. The error function $e = (e_{x_j},\ e_{y_j},\ e_{z_j})^T$ is described between the ith and the Nth oscillators, $j = 1,\ 2, \ldots,\ N-1;\ \alpha_i,\ i = 1,\ 2, \ldots,\ N$ represents the scaling factor of the ith system. The stable synchronization of mutually coupled N-oscillators for one of the state variables of the network system is defined by $x_1/\alpha_1 = x_2/\alpha_2 = \cdots = x_N/\alpha_N$ or it can be represented as $x_2 = (\alpha_2/\alpha_1)x_1,\ x_3 = (\alpha_3/\alpha_1)x_1, \ldots,\ x_N = (\alpha_N/\alpha_1)x_1$.

The signs of the non-zero constants α_i, $(i = 1, 2, \ldots, N)$ ensure the synchronization states whether it follows CS or AS. The ratios of the constants are said scaling factors which are used in the bidirectional coupling schemes for the network of oscillatory systems. The bidirectional coupling term has been considered as symmetric while $\alpha_1 = \alpha_2 = \cdots = \alpha_N$. We can reach only CS state when it is symmetric. The amplification and reduction in oscillators size are not occurred at this stage. The coupling term is considered as asymmetric while the constants are not equal. We can realize the CS and AS states at this stage. We can also observe the effect of asymmetric coupling terms in the oscillators behavior with amplification or reduction in size. The NOLC mechanism is shown by taking an example of $N = 4$ mutually coupled H-R neural oscillators at the parameter set $I = 3.3, r = 0.001, s = 4$. We design the four coupled identical H-R as follows:

$$\begin{aligned} \dot{x}_i &= y_i - x_i^3 + 3x_i^2 - z_i + I + W_{x_i}, \\ \dot{y}_i &= 1 - 5x_i^2 - y_i + W_{y_i}, \\ \dot{z}_i &= rs(x_i + 1.6) - rz_i + W_{z_i}, \end{aligned} \tag{45}$$

where $i = 1, 2, 3, 4$. The design of the oscillatory network system can be developed as follows. We first consider two H-R oscillators and create the NOLC based coupling to show that $\dot{V}(e) < 0$. Then, we add the third H-R oscillators and include the bidirectional coupling controller between the oscillators one and three, oscillators two and three to establish the LF stability criterion between the oscillators. Finally, we add one new oscillator to the network and consider the coupling technique between the oscillators one and four, oscillators two and four, oscillators three and four respectively. Now, we mathematically prove the synchronization for all the four coupled H-R oscillators.

Theorem. Consider the coupled network of H-R oscillators given by Eq. (45) which attains the desired synchronized state under the following controllers.

$$\begin{aligned} W_{x_i} &= \frac{p}{i(i-1)}(-e_{x_{i-1}} - e_{y_{i-1}} + e_{z_{i-1}}) + 3\left(1 - \frac{\alpha_i}{\alpha_1}\right)\frac{\alpha_i}{\alpha_1}x_1^2 + \left(-1 + \left(\frac{\alpha_i}{\alpha_1}\right)^2\right)\frac{\alpha_i}{\alpha_1}x_1^3 + I\left(-1 + \frac{\alpha_i}{\alpha_1}\right) \\ &\quad - \alpha_i \sum_{1 \le i < N} \frac{(-e_{x_i} - e_{y_i} + e_{z_i})}{(i+1)\alpha_{i+1}}, \\ W_{y_i} &= \left(-1 + \frac{\alpha_i}{\alpha_1}\right) + 5\left(-1 + \frac{\alpha_i}{\alpha_1}\right)\frac{\alpha_i}{\alpha_1}x_1^2, \\ W_{z_i} &= -\frac{p}{i(i-1)}(rse_{x_{i-1}}) + 1.6rs\left(-1 + \frac{\alpha_i}{\alpha_1}\right) + \alpha_i \sum_{1 \le i < N} \frac{(rse_{x_i})}{(i+1)\alpha_{i+1}}, \end{aligned} \tag{46}$$

where $i = 1, 2, 3, 4$ and $p = 0$ for $i = 1$ but $p = 1$ for $i > 1$.

Proof. First, we couple the two oscillators for $i = 1, 2$ and $N = 2$ while the error system is defined as

$$e_{x_1} = x_2 - (\alpha_2/\alpha_1)x_1,\ e_{y_1} = y_2 - (\alpha_2/\alpha_1)y_1,\ e_{z_1} = z_2 - (\alpha_2/\alpha_1)z_1. \tag{47}$$

Consider the Lyapunov function as

$$V = (1/2)(e_{x_1}^2 + e_{y_1}^2 + e_{z_1}^2), \tag{48}$$

$$\dot{V} = (e_{x_1}\dot{e}_{x_1} + e_{y_1}\dot{e}_{y_1} + e_{z_1}\dot{e}_{z_1}). \tag{49}$$

We assume that the synchronization is established. Therefore, substituting the values of $x_2 = (\alpha_2/\alpha_1)x_1$ and $y_2 = (\alpha_2/\alpha_1)y_1$ in Eq. (49), we have $\dot{V}(e) < 0$ to achieve the desired synchronous state. The mathematical formulation of the appropriate choice of coupling terms W_{x_i}, W_{y_i}, and W_{z_i} $(i = 1, 2)$ gives

$$\begin{aligned}
\dot{e}_{x_1} &= \dot{x}_2 - (\alpha_2/\alpha_1)\dot{x}_1 \\
&= (y_2 - x_2^3 + 3x_2^2 - z_2 + I + W_{x_2}) - (\alpha_2/\alpha_1)(y_1 - x_1^3 + 3x_1^2 - z_1 + I + W_{x_1}) \\
&= \{y_2 - x_2^3 + 3x_2^2 - z_2 + I + (1/2)(-e_{x_1} - e_{y_1} + e_{z_1}) + 3(1 - (\alpha_2/\alpha_1))(\alpha_2/\alpha_1)x_1^2 + (-1 + (\alpha_2/\alpha_1)^2)(\alpha_2/\alpha_1)x_1^3 \\
&\quad + I(-1 + (\alpha_2/\alpha_1))\} - (\alpha_2/\alpha_1)\{y_1 - x_1^3 + 3x_1^2 - z_1 \\
&\quad + I - (\alpha_1/2\alpha_2)(-e_{x_1} - e_{y_1} + e_{z_1})\} \\
&= e_{y_1} - e_{z_1} + (1/2)(-e_{x_1} - e_{y_1} + e_{z_1}) + (1/2)(-e_{x_1} - e_{y_1} + e_{z_1}) = -e_{x_1},
\end{aligned}$$

similarly,

$$\begin{aligned}
\dot{e}_{y_1} &= \dot{y}_2 - (\alpha_2/\alpha_1)\dot{y}_1 \\
&= (1 - 5x_2^2 - y_2 + W_{y_2}) - (\alpha_2/\alpha_1)(1 - 5x_1^2 - y_1 + W_{y_1}) \\
&= \{1 - 5x_2^2 - y_2 + (-1 + (\alpha_2/\alpha_1)) + 5(-1 + (\alpha_2/\alpha_1))(\alpha_2/\alpha_1)x_1^2\} - (\alpha_2/\alpha_1)(1 - 5x_1^2 - y_1) = -e_{y_1},
\end{aligned}$$

and

$$\begin{aligned}
\dot{e}_{z_1} &= \dot{z}_2 - (\alpha_2/\alpha_1)\dot{z}_1 \\
&= (rsx_2 + 1.6rs - rz_2 + W_{z_2}) - (\alpha_2/\alpha_1)(rsx_1 + 1.6rs - rz_1 + W_{z_1}) \\
&= \{rsx_2 + 1.6rs - rz_2 - (1/2)rse_{x_1} + 1.6rs(-1 + (\alpha_2/\alpha_1))\} \\
&\quad - (\alpha_2/\alpha_1)\{rsx_1 + 1.6rs - rz_1 + 1.6rs(-1 + (\alpha_2/\alpha_1)) + (\alpha_1/2\alpha_2)rse_{x_1}\} \\
&= rse_{x_1} - re_{z_1} - rse_{x_1} = -re_{z_1}.
\end{aligned}$$

Now, $\dot{V} = -(e_{x_1}^2 + e_{y_1}^2 + re_{z_1}^2) < 0$ as $0 < r < 1$.

Next, we add third oscillating system to the two coupled oscillators. The error system becomes

$$\begin{aligned}
e_{x_2} &= 2x_3 - \alpha_3((x_1/\alpha_1) + (x_2/\alpha_2)), \\
e_{y_2} &= 2y_3 - \alpha_3((y_1/\alpha_1) + (y_2/\alpha_2)), \\
e_{z_2} &= 2z_3 - \alpha_3((z_1/\alpha_1) + (z_2/\alpha_2)).
\end{aligned} \tag{50}$$

for $i = 1, 2, 3$ and $N = 3$. The Lyapunov function is considered as $V = (1/2)(e_{x_2}^2 + e_{y_2}^2 + e_{z_2}^2)$.

Assume the synchronization is achieved. We replace the values of $x_3 = (\alpha_3/\alpha_1)x_1$ and $y_3 = (\alpha_3/\alpha_1)y_1$ in the expression $\dot{V}(e)$ to attain stable synchronization for three oscillating system. The appropriate choice of coupling controllers W_{x_i}, W_{y_i}, and W_{z_i} $(i = 1, 2, 3)$ becomes

$$\begin{aligned}
\dot{e}_{x_2} &= 2\dot{x}_3 - (\alpha_3/\alpha_1)\dot{x}_1 - (\alpha_3/\alpha_2)\dot{x}_2 \\
&= 2(y_3 - x_3^3 + 3x_3^2 - z_3 + I + W_{x_3}) - (\alpha_3/\alpha_1)(y_1 - x_1^3 + 3x_1^2 - z_1 + I + W_{x_1}) \\
&\quad -(\alpha_3/\alpha_2)(y_2 - x_2^3 + 3x_2^2 - z_2 + I + W_{x_2}) \\
&= 2\{y_3 - x_3^3 + 3x_3^2 - z_3 + I + (1/6)(-e_{x_2} - e_{y_2} + e_{z_2}) + 3(1 - (\alpha_3/\alpha_1))(\alpha_3/\alpha_1)x_1^2 \\
&\quad +(-1 + (\alpha_3/\alpha_1)^2)(\alpha_3/\alpha_1)x_1^3 + I(-1 + (\alpha_3/\alpha_1))\} - (\alpha_3/\alpha_1)\{y_1 - x_1^3 + 3x_1^2 - z_1 + I \\
&\quad -(\alpha_1/2\alpha_2)(-e_{x_1} - e_{y_1} + e_{z_1}) - (\alpha_1/3\alpha_3)(-e_{x_2} - e_{y_2} + e_{z_2})\} - (\alpha_3/\alpha_2)\{y_2 - x_2^3 + 3x_2^2 - z_2 + I \\
&\quad +(1/2)(-e_{x_1} - e_{y_1} + e_{z_1}) + 3(1 - (\alpha_2/\alpha_1))(\alpha_2/\alpha_1)x_1^2 + (-1 + (\alpha_2/\alpha_1)^2)(\alpha_2/\alpha_1)x_1^3 \\
&\quad +I(-1 + (\alpha_2/\alpha_1)) - (\alpha_2/3\alpha_3)(-e_{x_2} - e_{y_2} + e_{z_2})\} \\
&= e_{y_2} - e_{z_2} + (-e_{x_2} - e_{y_2} + e_{z_2}) + (\alpha_3/2\alpha_2)(-e_{x_1} - e_{y_1} + e_{z_1}) - (\alpha_3/2\alpha_2)(-e_{x_1} - e_{y_1} + e_{z_1}) \\
&= -e_{x_2},
\end{aligned}$$

similarly,

$$\begin{aligned}
\dot{e}_{y_2} &= 2\dot{y}_3 - (\alpha_3/\alpha_1)\dot{y}_1 - (\alpha_3/\alpha_2)\dot{y}_2 \\
&= 2(1 - 5x_3^2 - y_3 + W_{y_3}) - (\alpha_3/\alpha_1)(1 - 5x_1^2 - y_1 + W_{y_1}) - (\alpha_3/\alpha_2)(1 - 5x_2^2 - y_2 + W_{y_2}) \\
&= 2\{1 - 5x_3^2 - y_3 + (-1 + (\alpha_3/\alpha_1)) + 5(-1 + (\alpha_3/\alpha_1))(\alpha_3/\alpha_1)x_1^2\} - (\alpha_3/\alpha_1)(1 - 5x_1^2 - y_1) \\
&\quad -(\alpha_3/\alpha_2)\{1 - 5x_2^2 - y_2 + (-1 + (\alpha_2/\alpha_1)) + 5(-1 + (\alpha_2/\alpha_1))(\alpha_2/\alpha_1)x_1^2\} = -e_{y_2}, \\
\dot{e}_{z_2} &= 2\dot{z}_3 - (\alpha_3/\alpha_1)\dot{z}_1 - (\alpha_3/\alpha_2)\dot{z}_2 \\
&= 2(rsx_3 + 1.6rs - rz_3 + W_{z_3}) - (\alpha_3/\alpha_1)(rsx_1 + 1.6rs - rz_1 + W_{z_1}) - (\alpha_3/\alpha_2)(rsx_2 + 1.6rs - rz_2 + W_{z_2}) \\
&= 2\{rsx_3 + 1.6rs - rz_3 - (1/6)rse_{x_2} + 1.6rs(-1 + (\alpha_3/\alpha_1))\} - (\alpha_3/\alpha_1)\{rsx_1 + 1.6rs - rz_1 \\
&\quad +(\alpha_1/2\alpha_2)rse_{x_1} + (\alpha_1/3\alpha_3)rse_{x_2}\} - (\alpha_3/\alpha_2)\{rsx_2 + 1.6rs - rz_2 - (1/2)rse_{x_1} + 1.6rs(-1 + (\alpha_2/\alpha_1)) \\
&\quad +(\alpha_2/3\alpha_3)rse_{x_2}\} = -re_{z_2}.
\end{aligned}$$

Now, the condition of synchronization is attained by using $\dot{V} = -(e_{x_2}^2 + e_{y_2}^2 + re_{z_2}^2) < 0$ and $0 < r < 1$. Finally, a fourth oscillator is added to the network of three oscillating system and the error functions for $i = 1, 2, 3, 4$ and $N = 4$ are represented as

$$\begin{aligned} e_{x_3} &= 3x_4 - \alpha_4((x_1/\alpha_1) + (x_2/\alpha_2) + (x_3/\alpha_3)), \\ e_{y_3} &= 3y_4 - \alpha_4((y_1/\alpha_1) + (y_2/\alpha_2) + (y_3/\alpha_3)), \\ e_{z_3} &= 3z_4 - \alpha_4((z_1/\alpha_1) + (z_2/\alpha_2) + (z_3/\alpha_3)). \end{aligned} \tag{51}$$

Consider the Lyapunov function as $V = (1/2)(e_{x_3}^2 + e_{y_3}^2 + e_{z_3}^2)$.

Assuming synchronization is established, we replace the values of the state variables $x_4 = (\alpha_4/\alpha_1)x_1$ and $y_4 = (\alpha_4/\alpha_1)y_1$ in the LF derivative $\dot{V}(e)$ to achieve the stable synchronization state in the network. The appropriate choice of coupling controllers W_{x_i}, W_{y_i}, and W_{z_i} $(i = 1, 2, 3, 4)$ becomes

$$\begin{aligned} \dot{e}_{x_3} &= 3\dot{x}_4 - (\alpha_4/\alpha_1)\dot{x}_1 - (\alpha_4/\alpha_2)\dot{x}_2 - (\alpha_4/\alpha_3)\dot{x}_3 \\ &= 3(y_4 - x_4^3 + 3x_4^2 - z_4 + I + W_{x_4}) - (\alpha_4/\alpha_1)(y_1 - x_1^3 + 3x_1^2 - z_1 + I + W_{x_1}) \\ &\quad -(\alpha_4/\alpha_2)(y_2 - x_2^3 + 3x_2^2 - z_2 + I + W_{x_2}) - (\alpha_4/\alpha_3)(y_3 - x_3^3 + 3x_3^2 - z_3 + I + W_{x_3}) \\ &= 3\{y_4 - x_4^3 + 3x_4^2 - z_4 + I + (1/12)(-e_{x_3} - e_{y_3} + e_{z_3}) + 3(1 - (\alpha_4/\alpha_1))(\alpha_4/\alpha_1)x_1^2 \\ &\quad +(-1 + (\alpha_4/\alpha_1)^2)(\alpha_4/\alpha_1)x_1^3 + I(-1 + (\alpha_4/\alpha_1))\} - (\alpha_4/\alpha_1)\{y_1 - x_1^3 + 3x_1^2 - z_1 + I \\ &\quad -(\alpha_1/2\alpha_2)(-e_{x_1} - e_{y_1} + e_{z_1}) - (\alpha_1/3\alpha_3)(-e_{x_2} - e_{y_2} + e_{z_2}) - (\alpha_1/4\alpha_4)(-e_{x_3} - e_{y_3} + e_{z_3})\} \\ &\quad -(\alpha_4/\alpha_2)\{y_2 - x_2^3 + 3x_2^2 - z_2 + I + (1/2)(-e_{x_1} - e_{y_1} + e_{z_1}) + 3(1 - (\alpha_2/\alpha_1))(\alpha_2/\alpha_1)x_1^2 \\ &\quad +(-1 + (\alpha_2/\alpha_1)^2)(\alpha_2/\alpha_1)x_1^3 + I(-1 + (\alpha_2/\alpha_1)) - (\alpha_2/3\alpha_3)(-e_{x_2} - e_{y_2} + e_{z_2}) \\ &\quad -(\alpha_2/4\alpha_4)(-e_{x_3} - e_{y_3} + e_{z_3})\} - (\alpha_4/\alpha_3)\{y_3 - x_3^3 + 3x_3^2 - z_3 + I + (1/6)(-e_{x_2} - e_{y_2} + e_{z_2}) \\ &\quad +3(1 - (\alpha_3/\alpha_1))(\alpha_3/\alpha_1)x_1^2 + (-1 + (\alpha_3/\alpha_1)^2)(\alpha_3/\alpha_1)x_1^3 + I(-1 + (\alpha_3/\alpha_1)) \\ &\quad -(\alpha_3/4\alpha_4)(-e_{x_3} - e_{y_3} + e_{z_3})\} \\ &= e_{y_3} - e_{z_3} - (1/4 + 1/4 + 1/4 + 1/4)(-e_{x_3} - e_{y_3} + e_{z_3}) + (\alpha_4/2\alpha_3)(-e_{x_2} - e_{y_2} + e_{z_2}) \\ &\quad +(\alpha_4/2\alpha_2)(-e_{x_1} - e_{y_1} + e_{z_1}) - (\alpha_4/2\alpha_2)(-e_{x_1} - e_{y_1} + e_{z_1}) \\ &= -e_{x_3}, \end{aligned}$$

$$\begin{aligned} \dot{e}_{y_3} &= 3\dot{y}_4 - (\alpha_4/\alpha_1)\dot{y}_1 - (\alpha_4/\alpha_2)\dot{y}_2 - (\alpha_4/\alpha_3)\dot{y}_3 \\ &= 3(1 - 5x_4^2 - y_4 + W_{y_4}) - (\alpha_4/\alpha_1)(1 - 5x_1^2 - y_1 + W_{y_1}) - (\alpha_4/\alpha_2)(1 - 5x_2^2 - y_2 + W_{y_2}) \\ &\quad -(\alpha_4/\alpha_3)(1 - 5x_3^2 - y_3 + W_{y_3}) \\ &= 3\{1 - 5x_4^2 - y_4 + (-1 + (\alpha_4/\alpha_1)) + 5(-1 + (\alpha_4/\alpha_1))(\alpha_4/\alpha_1)x_1^2\} - (\alpha_4/\alpha_1)(1 - 5x_1^2 - y_1) \\ &\quad -(\alpha_4/\alpha_2)\{1 - 5x_2^2 - y_2 + (-1 + (\alpha_2/\alpha_1)) + 5(-1 + (\alpha_2/\alpha_1))(\alpha_2/\alpha_1)x_1^2\} \\ &\quad -(\alpha_4/\alpha_3)\{1 - 5x_3^2 - y_3 + (-1 + (\alpha_3/\alpha_1)) + 5(-1 + (\alpha_3/\alpha_1))(\alpha_3/\alpha_1)x_1^2\} \\ &= -e_{y_3} + 3(\alpha_4/\alpha_1) - 3(\alpha_4/\alpha_1)(5x_1^2) - (\alpha_4/\alpha_1) + 5(\alpha_4/\alpha_1)x_1^2 - (\alpha_4/\alpha_2)(\alpha_2/\alpha_1) \\ &\quad +(\alpha_4/\alpha_2)(\alpha_2/\alpha_1)(5x_1^2) - (\alpha_4/\alpha_3)(\alpha_3/\alpha_1) + (\alpha_4/\alpha_3)(\alpha_3/\alpha_1)(5x_1^2) = -e_{y_3}, \end{aligned}$$

and

$$\begin{aligned} \dot{e}_{z_3} &= 3\dot{z}_4 - (\alpha_4/\alpha_1)\dot{z}_1 - (\alpha_4/\alpha_2)\dot{z}_2 - (\alpha_4/\alpha_3)\dot{z}_3 \\ &= 3(rsx_4 + 1.6rs - rz_4 + W_{z_4}) - (\alpha_4/\alpha_1)(rsx_1 + 1.6rs - rz_1 + W_{z_1}) - (\alpha_4/\alpha_2)(rsx_2 + 1.6rs - rz_2 + W_{z_2}) \\ &\quad -(\alpha_4/\alpha_3)(rsx_3 + 1.6rs - rz_3 + W_{z_3}) \\ &= 3\{rsx_4 + 1.6rs - rz_4 - (1/12)rse_{x_3} + 1.6rs(-1 + (\alpha_4/\alpha_1))\} - (\alpha_4/\alpha_1)\{rsx_1 + 1.6rs - rz_1 \\ &\quad +(\alpha_1/2\alpha_2)rse_{x_1} + (\alpha_1/3\alpha_3)rse_{x_2} + (\alpha_1/4\alpha_4)rse_{x_3}\} - (\alpha_4/\alpha_2)\{rsx_2 + 1.6rs - rz_2 - (1/2)rse_{x_1} \\ &\quad +1.6rs(-1 + (\alpha_2/\alpha_1)) + (\alpha_2/3\alpha_3)rse_{x_2} + (\alpha_2/4\alpha_4)rse_{x_3}\} - (\alpha_4/\alpha_3)\{rsx_3 + 1.6rs - rz_3 \\ &\quad -(1/6)rse_{x_2} + 1.6rs(-1 + (\alpha_3/\alpha_1)) + (\alpha_3/4\alpha_4)rse_{x_3}\} \\ &= rse_{x_3} - re_{z_3} - (1/4 + 1/4 + 1/4 + 1/4)rse_{x_3} - (\alpha_4/2\alpha_2)rse_{x_1} + (\alpha_4/2\alpha_2)rse_{x_1} - (5\alpha_4/6\alpha_2)rse_{x_2} \\ &= -re_{z_3}. \end{aligned}$$

We replace the values of the system variables $x_3 = (\alpha_3/\alpha_1)x_1$ and $y_3 = (\alpha_3/\alpha_1)y_1$ and $z_3 = (\alpha_3/\alpha_1)z_1$ for the network of three H-R oscillators to establish the synchronization. Therefore, $\lim_{t\to\infty} \|e\| \to 0$. Thus, we can derive the error systems of bidirectionally coupled N oscillatory systems in the above mentioned procedure to check the stability of desired synchronous state.□

First, we assume that the network contains two identical coupled oscillator systems and the remaining oscillators are uncoupled. We choose $\alpha_1 = 1$, $\alpha_2 = 1$ for the synchronous behavior of identical coupled H-R oscillator systems. Now, we add the third oscillating system to the network and take $\alpha_1 = 1$, $\alpha_2 = 1$, $\alpha_3 = -1$. The third identical oscillating system is inverted to both the first and second oscillating systems. The first and second oscillating systems remain in CS state but the third oscillating system shows AS with both the first and second oscillating system. Finally, we consider the fourth identical H-R oscillating system and choose $\alpha_1 = 1$, $\alpha_2 = 1$, $\alpha_3 = -1$, $\alpha_4 = 1$. The fourth oscillating system shows CS with first and second oscillating systems and AS with the third oscillating system and it has been presented in Fig. 9a and b.

The design of the above proposed coupling technique ensures the required synchronization states. In this method, the oscillators can be amplified or it can reduce the size for appropriately chosen scaling factors $\alpha_1, \alpha_2, \alpha_3$ and α_4. The scaling factors take suitable negative and positive values to reach both CS and AS regimes. Now, we consider the four H-R oscillators with the same NOLC based bidirectional coupling at the parameter values (i) $I = 3.05, r = 0.005, s = 4$ with suitable scaling factors $\alpha_1 = 1$, $\alpha_2 = 3$, $\alpha_3 = 1$, $\alpha_4 = 4$ and (ii) $I = 1.345, r = 0.001, s = 4$ with appropriate scaling factors $\alpha_1 = 4$, $\alpha_2 = 1$, $\alpha_3 = -1$, $\alpha_4 = 2$ to achieve the desired synchronous states (Figs. 10b and d) and it also presents the am-

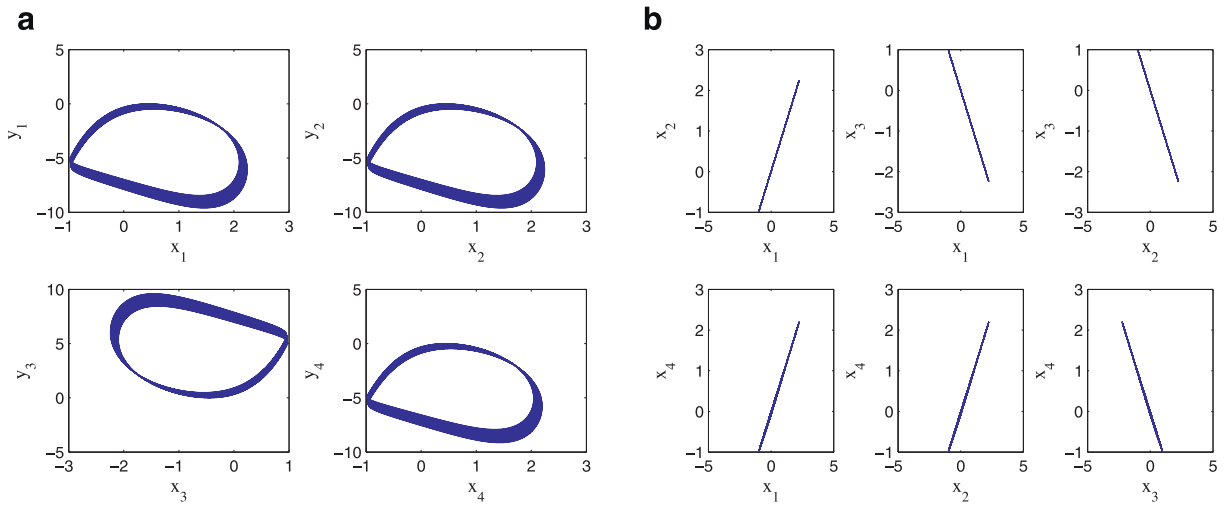

Fig. 9. Two dimensional phase diagrams of a network of four bidirectionally coupled identical H-R neural oscillators and the CS-AS states after synchronization.

plification and reduction in size of the coupled oscillators (Fig. 10a and c). Thus, the coupling mechanism is constructed and the desired synchronization is shown in a network of four coupled identical H-R oscillating system. In the similar manner, we can extend the coupling technique for a network of N-oscillating systems to achieve the desired synchronous state.

The desired synchronization is achieved by the LF stability condition and we only show the results for the synchronization state at a particular set of parameter values for the coupling scheme and other results follow the same type behavior for suitable parameters and coupling coefficients. The illustrated results verify the coupling technique and effectiveness of the proposed method. Consider the ring type bidirectionally coupled network of N oscillators as follows:

$$\begin{cases} \dot{U}_1 = AU_1 + f(U_1) + d_1(U_2 + U_N - 2U_1), \\ \dot{U}_2 = AU_2 + f(U_2) + d_2(U_1 + U_3 - 2U_2), \\ \qquad\qquad \vdots \\ \dot{U}_{N-1} = AU_{N-1} + f(U_{N-1}) + d_{N-1}(U_{N-2} + U_N - 2U_{N-1}), \\ \dot{U}_N = AU_N + f(U_N) + d_N(U_{N-1} + U_1 - 2U_N), \end{cases} \tag{52}$$

where the system state vectors are represented as $(U_1,\ U_2, \ldots,\ U_N) \in R^n$ and $N > 2$. The coupling coefficients are represented as the diagonal matrix $d_i = diag(d_{1k},\ d_{2k}, \ldots,\ d_{Nk})$ for $d_{ik} \geq 0$. The error functions are defined as $e_i = U_i - U_{i+1},\ (i = 1,\ 2, \ldots,\ N-1)$. The network systems reach the synchronous state for suitable values of $d_i \geq 0$ as $\lim_{t\to\infty} \|e_i\| = 0,\ (i = 1,\ 2, \ldots,\ N-1)$. Consider $U_i = (x_i,\ y_i,\ z_i)$ for $i = 1, 2, 3, 4$. The network of $N = 4$, H-R oscillators with the ring type network connection can be described as follows:

$$\begin{pmatrix} \dot{x}_i \\ \dot{y}_i \\ \dot{z}_i \end{pmatrix} = \begin{pmatrix} 0 & 1 & -1 \\ 0 & -1 & 0 \\ rs & 0 & -r \end{pmatrix} \begin{pmatrix} x_i \\ y_i \\ z_i \end{pmatrix} + \begin{pmatrix} -x_i^3 + 3x_i^2 \\ 1 - 5x_i^2 \\ 1.6rs \end{pmatrix} + \begin{pmatrix} d_{i1} & 0 & 0 \\ 0 & d_{i2} & 0 \\ 0 & 0 & d_{i3} \end{pmatrix} (g(U_1, U_2, ..., U_N))_{3\times 1}. \tag{53}$$

To reach the desired synchronous state, we consider the set of parameters as $I = 3.3, r = 0.001, s = 4,\ N = 4$ for periodic spiking and all the coupling coefficients equal to one. By using the above parameter values and coupling coefficients, the network of oscillators reach the targeted synchronized state (see Fig. 11a and b) . We have derived the result for one set of parameters. However, it can also be presented for other set of parameters and for appropriate coupling coefficients.

The complex behavior of network connections and coupling functions for synchronization present significant results and have importance in clinical research. The spiking and different types of bursting measure the characteristics and nonlinear phenomena of the neurons [28,35,37]. The synchronized firing of the network of biological oscillators are relevant in information transmission and coding. Some different types of neural network structures and its synchronization were studied in the references [40–42]. However, it is not completely known the types of coupling connections and the appropriate parameters for a neural network of oscillators. The synchronous behavior of a bursting neural network depends on the network structure [40], coupling controllers and coupling coefficients.

5. Conclusions

In this paper, we produce the generalized synchronization (GS) state between a driver-response neural systems. The coupling technique is expressed as various types of transformation matrices which map a driver system into a response

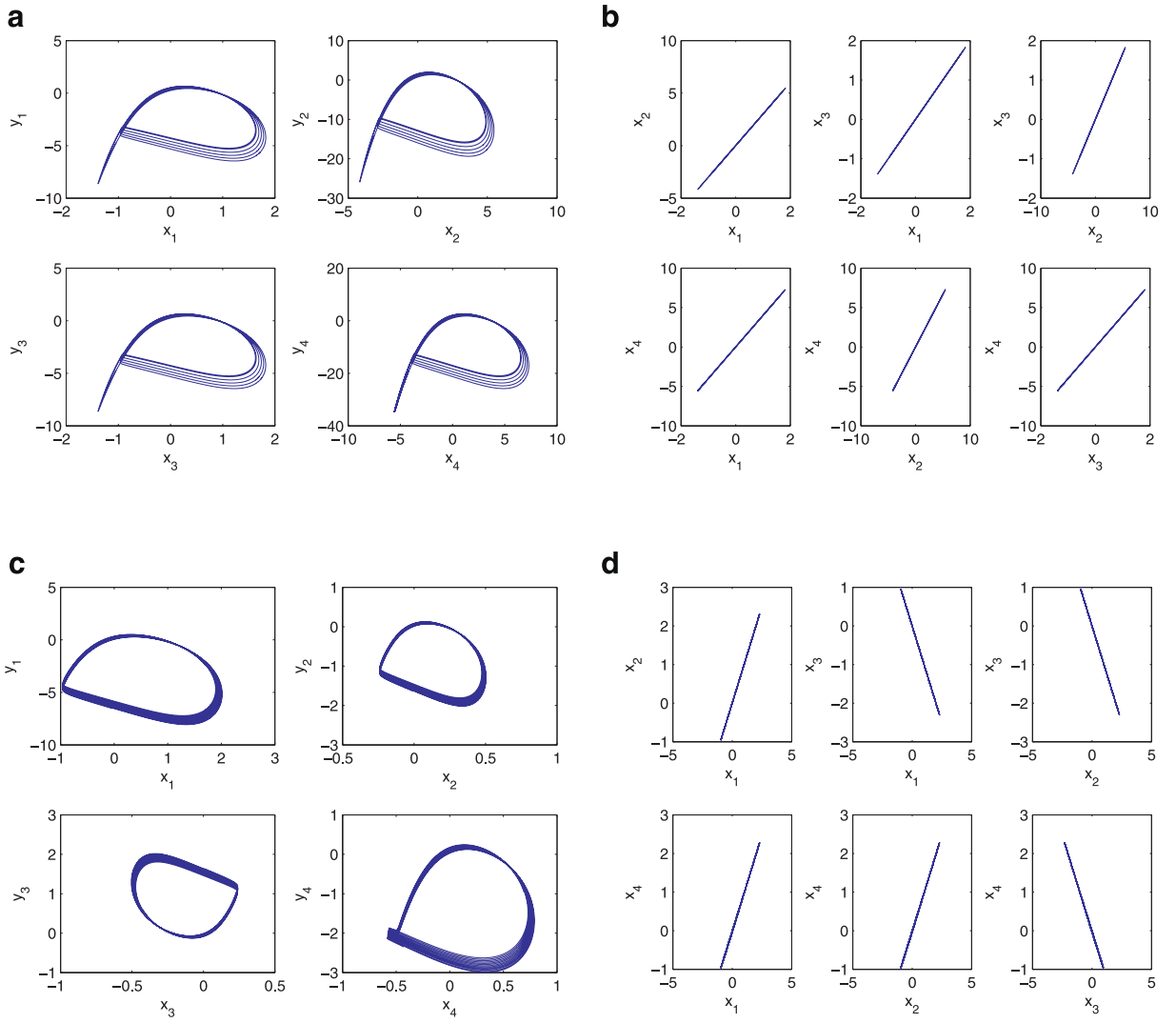

Fig. 10. CS and AS states of a network of four bidirectionally coupled identical H-R oscillators after synchronization at parameter sets $I = 3.05, r = 0.005, s = 4$ and $I = 1.345, r = 0.001, s = 4$ respectively.

system. The method is also applicable when the transformation matrix is completely different and explained as variables of other dynamical systems. We explained the applications of the coupling scheme for several types of transformation matrices such as constants, periodic functions, state variables of the driver system.

Two numerical examples of modified Morris–Lecar (M-L) model and bursting M-L model are presented to illustrate the open-plus-closed-loop (OPCL) coupling scheme for two non-identical neural oscillators. We observe that the transformation of the target (i.e., driven system) is necessary to have complete correlation between both driver and response systems.

We also investigate a nonlinear open loop controller (NOLC) based bidirectional coupling mechanism through Lyapunov function stability criterion and able to show the complete (CS) and anti-synchronization (AS) in a network of H-R neural model systems. We remark that a multiplicative factor (scaling factor α in our case) is responsible for amplification or attenuation of one neural oscillating system to other. We present the theory of bidirectional coupling to the network of four H-R neural oscillating systems, and consider comparable coupling technique using bidirectional ring type connections. The illustrated results verify our coupling scheme and effectiveness of the proposed method.

The method can be extended for N network of model neurons to produce the desired synchronous behavior. As a real world application of this work, we consider some situation in some diseases, we need to control the oscillations of neurons in some area of the brain. Then, by injecting the drug or current to make those oscillations going towards desired target (like $g(t)$ in our case) which will be constrained in such a way that it will perform the required dynamics.

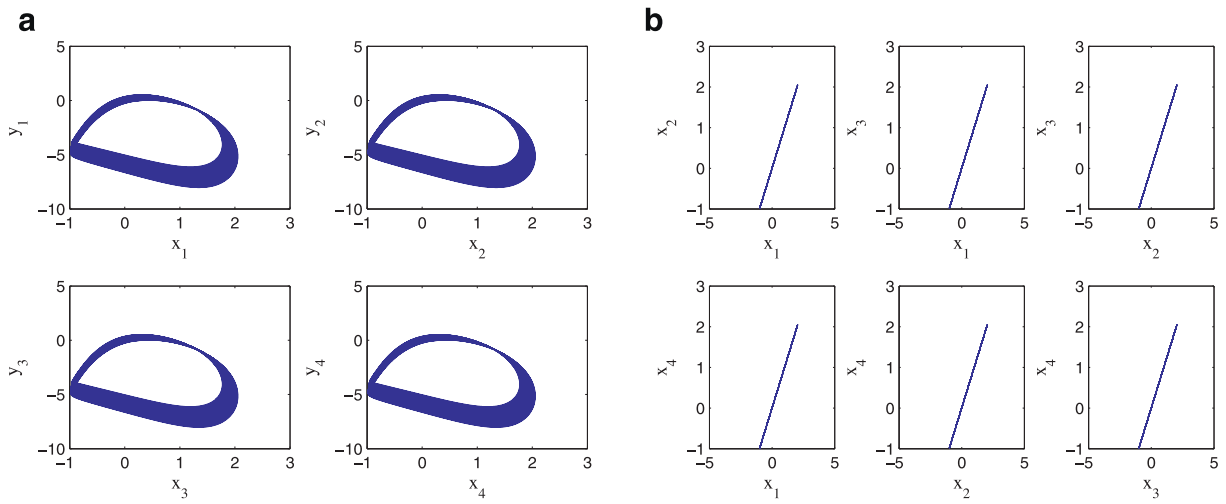

Fig. 11. CS states of a network of four bidirectionally coupled (ring type connection) identical H-R neural oscillators after synchronization at the parameter set $I = 3.3, r = 0.001, s = 4$.

Acknowledgments

The authors are very much thankful to the handling subject Editor and Reviewer for their valuable and constructive suggestions on the manuscript.

References

[1] A.S. Pikovsky, M.G. Rosenblum, J. Kurths, Synchronization: A concept in Nonlinear Sciences, CUP, New York, 2001.
[2] S. Boccaletti, J. Kurths, G. Osipov, D.L. Valladares, C. Zhou, The synchronization of chaotic systems, Phys. Rep. 366 (2002) 1–101.
[3] S.K. Dana, P.K. Roy, J. Kurths, Complex Dynamics in Physiological Systems: From Heart to Brain, Complexity Series, Springer, New York, 2008.
[4] P.J. Uhlhaas, W. Singer, Neural synchrony in brain disorders: Relevance for cognitive dysfunctions and pathophysiology, Neuron 52 (2006) 155–168.
[5] M.G. Rosenblum, A.S. Pikovsky, Controlling synchronization in a ensemble of globally coupled oscillators, Phys. Rev. Lett. 92 (2004) 114102.
[6] J. Mayer, H.G. Schuster, J.C. Claussen, M. Molle, Corticothalamic projections control synchronization in locally coupled bistable thalamic oscillators, Phys. Rev. Lett. 99 (2007) 068102.
[7] O.V. Popovych, C. Hauptmann, P.A. Tass, Effective desynchronization by nonlinear delayed feedback, Phys. Rev. Lett. 94 (2005) 164102.
[8] E.A. Jackson, I. Grosu, An open-plus-closed-loop (OPCL) control of complex dynamic systems, Physica D 85 (1995) 1–9.
[9] I. Grosu, Robust synchronization, Phys. Rev. E 56 (1997) 3709.
[10] H. Fujisaka, T. Yamada, Stability theory of synchronized motion in coupled oscillator systems, Prog. Theor. Phys. 69 (1983) 32–47.
[11] L.M. Pecora, T. Carroll, Synchronization in chaotic systems, Phys. Rev. Lett. 64 (1990) 821–824.
[12] L.Y. Cao, Y.C. Lai, Antiphase synchronization in chaotic systems, Phys. Rev. E 58 (1998) 382–386.
[13] W. Liu, J. Xiao, X. Qian, J. Yang, Antiphase synchronization in coupled chaotic oscillators, Phys. Rev. E 73 (2006) 057203.
[14] M. Rosenblum, A.S. Pikovsky, J. Kurths, Phase synchronization in chaotic oscillators, Phys. Rev. Lett. 76 (1996) 1804.
[15] S.K. Dana, B. Blasius, J. Kurths, Experimental evidence of anomalous phase synchronization in two diffusively coupled chen oscillators, Chaos 16 (2006) 023111.
[16] N.F. Rulkov, M.M. Suschik, L.S. Tsimring, H.D.I. Abarbanel, Generalized synchronization of chaos in directionally coupled chaotic systems, Phys. Rev. E 51 (1995) 980–994.
[17] A.E. Hramov, A.A. Koronovskii, Generalized synchronization, Phys. Rev. E 71 (2005) 067201.
[18] P.K. Roy, C. Hens, I. Grosu, S.K. Dana, Engineering generalized synchronization in chaotic oscillators, Chaos 21 (2011) 013106.
[19] M. Rosenblum, A.S. Pikovsky, J. Kurths, From phase to lag synchronization in coupled chaotic oscillators, Phys. Rev. Lett. 78 (1997) 4193.
[20] S. Taherion, Y.C. Lai, Observability of lag synchronization of coupled chaotic oscillators, Phys. Rev. E 59 (1999) R6247.
[21] A.E. Hramov, A.A. Koronovskii, Time scale synchronization of chaotic oscillators, Physica D 206 (2005) 252–264.
[22] T. Tateno, K. Pakdaman, Random dynamics of the Morris–Lecar neural model, Chaos 14 (2004) 511–530.
[23] C. Morris, H. Lecar, Voltage oscillations in the barnacle muscle fiber, J. Biophys. 35 (1981) 193–213.
[24] B.S. Gutkin, G.B. Ermentrout, Dynamics of membrane excitability determine interspike interval variability: a link between spike generation mechanisms and cortical spike train statics, Neural Comput. 10 (1998) 1047–1065.
[25] Y. Xie, J.X. Xu, S.J. Hu, A novel dynamical mechanism of neural excitability for integer multiple spiking, Chaos Solitons Fractals 21 (2004) 177–184.
[26] R. Larter, B. Speelman, R.M. Worth, A coupled ordinary differential equation lattice model for the simulation of epileptic seizures, Chaos 9 (1999) 795–804.
[27] S.R. Nadar, V. Rai, Transient periodicity in a Morris–Lecar neural system, ISRN Biomathematics 2012 (2012) 1–7.
[28] E.M. Izhikevich, Neural excitability, spiking and bursting, Int. J. Bifur. Chaos 10 (2000) 1171–1266.
[29] M. Shi, Z. Wang, Abundant bursting patterns of a fractional-order Morris–Lecar neuron model, Commun. Nonlinear Sci. Numer. Simulat. 19 (2014) 1956–1969.
[30] F.K. Skinner, L. Zhang, J.L.P. Velazquez, P.L. Carlen, Bursting in inhibitory interneuronal networks: a role for gap-junctional coupling, J. Neurophysiol. 81 (1999) 1274–1283.
[31] M. Breakspeara, J.R. Terry, K.J. Friston, Modulation of excitatory synaptic coupling facilitates synchronization and complex dynamics in a nonlinear model of neuronal dynamics, Neurocomputing 52–54 (2003) 151–158.
[32] S.G. Hormuzdi, M.A. Filippov, G. Mitropoulou, H. Monyer, R. Bruzzone, Electrical synapses: a dynamic signaling system that shapes the activity of neuronal networks, BBA 1662 (2004) 113–137.
[33] J.L. Hindmarsh, R.M. Rose, A mode of the nerve impulse using two first-order differential equation, Nature (London) 296 (1982) 162–164.

[34] J.L. Hindmarsh, R.M. Rose, A model of neuronal bursting using three coupled first order differential equations, Philos. Trans. R. Soc. London B. Biol. Sci. 221 (1984) 87–102.
[35] E.M. Izhikevich, Which model to use for cortical spiking neurons, IEEE Trans. Neural Netw. 15 (2004) 1063–1067.
[36] N. Corson, M.A. Aziz-Alaoui, Asymptotic dynamics of Hindmarsh–Rose neuronal system, Dyn. Contin. Discret. Impuls. Syst. Ser. B, 16 (2009) 535–549.
[37] S.R.D. Djeundam, R. Yamapi, T.C. Kofane, M.A. Aziz-Alaoui, Deterministic and stochastic bifurcations in the Hindmarsh–Rose neuronal model with and without random signal, Chaos 23 (2013) 033125.
[38] R. Mainieri, J. Rehacek, Projective synchronization in three-dimensional chaotic systems, Phys. Rev. Lett. 82 (1999) 3042.
[39] E. Padmanaban, C. Hens, S.K. Dana, Engineering synchronization of chaotic oscillators using controller based coupling design, Chaos 21 (2011) 013110.
[40] I. Belykh, E. De Lange, M. Hasler, Synchronization of bursting neurons: what matters in the network topology, Phys. Rev. Lett. 94 (2005) 188101.
[41] Y. Tang, J. Fang, Synchronization of *n*-coupled fractional -order chaotic systems with ring connection, Commun. Nonlinear Sci. Numer. Simulat. 15 (2010) 401–412.
[42] F.J. Jhou, J. Juang, Y.H. Liang, Multistate and multistage synchronization of Hindmarsh–Rose neurons with excitatory and electrical synapses, IEEE Trans. Cir. Syst. 59 (2012) 1335–1347.
[43] I. Grosu, E. Padmanaban, P.K. Roy, S.K. Dana, Designing coupling for synchronization and amplification of chaos, Phys. Rev. Lett. 100 (2008) 234102.
[44] I. Grosu, R. Banerjee, P.K. Roy, S.K. Dana, Design of coupling for synchronization of chaotic oscillators, Phys. Rev. E 80 (2009) 016212.
[45] H.X. Wang, Q.Y. Wang, Q.S. Lu, Bursting and synchronization transition in the coupled modified ML neurons, Commun. Nonlinear Sci. Numer. Simul. 13 (2008) 1668–1675.
[46] R. FitzHugh, Impulses and physiological states in theoretical models of nerve membrane, Biophys. J. 1 (1961) 445–466.